~~Thermodynamic evolution of a finite~~ Analytical solutions for the advective-diffusive ice column ~~: analytical solution and basal-melting timescales~~in the presence of strain heating

Daniel Moreno-Parada[1,2], Alexander Robinson[1,2], Marisa Montoya[1,2], and Jorge Alvarez-Solas[1,2]

[1]Departamento de Física de la Tierra y Astrofísica, Universidad Complutense de Madrid, Facultad de Ciencias Físicas, 28040 Madrid, Spain
[2]Instituto de Geociencias, Consejo Superior de Investigaciones Cientifícas-Universidad Complutense de Madrid, 28040 Madrid, Spain

Correspondence: Daniel Moreno-Parada (danielm@ucm.es)

Abstract. ~~The temperature distribution in ice sheets is worthy of attention given the strong relation with ice dynamics and the intrinsic information about past surface temperature variations. Here we refine the classical analysis of free oscillations in an ice sheet by analytically solving the thermal evolution of an ice column. In so doing, we provide analytical solutions to the one-dimensional Fourier heat equation over a finite motionless ice column for a more general (Robin) boundary condition problem. The time evolution of the temperature profiles appears to be strongly dependent on the column thickness L and largely differs from previous studies that assumed an infinite column thickness. Consequently, the time required for the column base to thaw depends on several factors besides the ice thermal properties:~~ A thorough understanding of ice thermodynamics is of paramount importance if an accurate description of glaciers, ice sheets and ice shelves is to be found. Yet there exists a significant gap in our theoretical knowledge of the time-dependent behaviour of ice temperatures due to the inevitable compromise between mathematical tractability and the accurate depiction of physical phenomena. In order to bridge this shortfall, we have analytically solved the 1D time-dependent advective-diffusive heat problem including a source term due to strain heating and a sophisticated top boundary condition (Robin type) that considers potential non-equilibrium thermal states across the ice-air interface. The solution is expressed in terms of confluent hypergeometric functions following a separation of variables approach. Non-dimensionalisation reduces the parameter space to four numbers that fully determine the shape of the solution at equilibrium: surface insulation, effective geothermal heat flow, the Peclét number and the Brikman number. Nevertheless, the transient component is mostly determined by the Peclét number and the effective heat flux parameter, while the initial temperature ~~profile, the boundary conditions and the ice-column thickness L. This timescale is classically considered to be the period of a binge-purge oscillator, a potential mechanism behind the Heinrich Events. Our analytical solutions show a broad range of periods for typical-size column thicknesses. In the limit $L \to \infty$, the particular valuesof the prescribed temperature at the top of the column become irrelevant and the reference value of ~ 7000 years, previously estimated for an idealised infinite domain, is retrieved. More generally, we prove that solutions with different upper boundary conditions, covered by our formulation, converge to the same result in such a limit. These results ultimately illustrate a subtle connection between internal free (the binge-purge hypothesis) and externally-driven (a time-dependent boundary condition at~~

the top) mechanisms caused by the finitude of the domain. Since thermomechanical instabilities (i.e., the transition between two plausible modes of basal lubrication governed by the thermal state of the ice) are the triggering mechanism of a binge-purge oscillator, internal free oscillations are sensitive to the particular climatic forcing imposed as a boundary condition at the top of the ice column. Lastly, analytical distribution exponentially converges to the stationary solution. The particular top boundary condition appears to be essential for the upwards advective scenario, thus yielding warmer temperatures in the entire column with increasing intensity as the geothermal heat flux takes higher values. On the contrary, temperature profiles are completely independent of the surface insulation for the downwards counterpart. A further energy content study of the transient component reveals that the downwards scenario exchanges energy at a higher rate than the upwards advective case, leading to faster convergence to the equilibrium thermal state. We have extended our study to a broader range of vertical dependency of the advective term, unlike prior studies limited to linear and quadratic profiles. Results show that the exponent $m = 3/2$ best describes benchmark experiments (e.g., EISMINT) vertical velocities and is therefore applicable as an independent analytical control on the temperature. The solutions presented herein are applicable in any context where our Robin boundary problem is satisfiedgeneral and fully applicable to any problem with an equivalent set of boundary conditions and any given initial temperature distribution. Analytical results of this work additionally provide refined benchmark solutions to test thermomechanical models.

1 Introduction

Periodic episodes of extreme iceberg discharge have captivated the glaciological and palaeoclimatological community for The study of ice thermodynamics is of crucial importance for understanding the behaviour of glaciers, ice sheets and ice shelves, as their evolution is strongly dependent on the physical properties of the last three decades. Yet the ultimate cause of these so-called Heinrich Events (HE) remains elusive. Several mechanisms have been proposed in the literature that can be broadly classified into two branches: internal free and externally-driven oscillations.

Free oscillations were first proposed in MacAyeal (1993a) as manifestations of the Laurentide Ice Sheet (LIS) purging excess ice volume. This interpretation rests on the assumption that a transition exists between two potential states of basal lubrication (Alley and Whillans, 1991; Hughes, 1992) and it is known as the binge-purge hypothesis. Namely, when the basal icetemperature is below the pressure melting point, the ice sheet is assumed to be stagnant and it simply thickens due to snow accumulation. As a result of the geothermal heat flow, the ice column is expected to warm and the base eventually yields melting. At this point, the icesheet is no longer at rest and begins to slide over a lubricated sediment bed. The purge phase continuous until the basal temperature gradient exceeds the value that can be maintained by . Ice thermodynamics is the geothermal heat flux and the frictional energy dissipation combined. MacAyeal (1993a) thus investigated what causes the bed of the LIS in Hudson Bay and Hudson Strait to shift from a frozen to a thawed state as well as the time length involved in this

process. To this end, he developed a conceptual model that shows how amplitude and periodicity depend on two environmental factors: the annual average sea-level temperature and the atmospheric lapse rate (MacAyeal, 1993a). Furthermore, a periodicity of $T \approx 7000$ years was estimated from these two factors for a simplified geometry. This value was determined as the time required for the base of a semi-infinite one-dimensional motionless ice column to reach the melting point due to a constant geothermal heat flow (analytically from Carslaw and Jaeger, 1988) and it marks the onset of the purge phase on a binge-purge cycle. The absence of time dependent boundary conditions throughout the study is noteworthy. result of a complex interplay between advection, diffusion and various heat sources. Only an accurate representation of these processes will allow for a robust description of ice flow, mass balance and overall stability. In this context, the development of analytical solutions for ice thermodynamics can provide deeper comprehension of the fundamental physics of ice, as they are intuitively interpretable, reveal hidden symmetries and further serve as a verification tool of numerical models.

Even though both the period and amplitude of the free oscillations appear to be dependent on environmental factors, the same study dismissed the possibility of an oscillation period imposed by an external harmonic atmospheric forcing as a result of the strong amplitude attenuation with depth. In other words, if such a periodic external climate forcing did exist, its imprint would be negligible at the base of the ice sheet. To prove so, MacAyeal (1993a) showed that the corresponding e-folding decay length of a $T \approx 7000$ years periodicity reads $\sqrt{2k/\omega} = 314$ m for a motionless ice column. Moreover, a constant vertical velocity was also considered so as to account for a potential advection term, thus increasing the e-folding decay length to 970 m. In view of these results, it is evident that a harmonic surface temperature fluctuation would become negligible at the base of a thick ice sheet. Robin (1955) and Lliboutry (1963) first laid the groundwork for understanding ice-column thermodynamics in the presence of vertical advection by providing analytical solutions for the stationary cases. These seminal works offered valuable insights into the steady-state behaviour of ice columns subject to advective-diffusive processes. Nevertheless, they did not consider the time-dependent evolution of ice temperatures. Hence, their applicability was limited to situations involving steady-state ice flow and fixed environmental conditions.

To provide quantitative support to the conceptual model, a low-order model of the HE cycle was additionally developed (MacAyeal, 1993b) to confirm that In a broader context, the theoretical estimation of HE periodicity T is in fact determined by the aforementioned environmental factors (MacAyeal, 1993a). In this two-dimensional model, iceflow mechanics and mass balance are combined in a manner that yields null horizontal ice flow when the base is frozen whereas deforming sediments allow for rapid sliding when the base is melted. Internal ice deformation is disregarded and ice thickness is assumed to be uniform along the cross section of the LIS (from Hudson Bay to the mouth of Hudson Strait). Remarkably, the numerical periodicity showed a discrepancy from the theoretical estimation of solely 4%.However, this relaxation oscillator model assumes a characteristic ice stream purge timescale of 250 years, given the absence of explicit simulations of a Hudson Strait ice stream. Notably, this choice is relevant for the long timescale of the HE since it determines the switch from purge to growth behaviour, found to be 450 years in the numerical results. 1D advective-diffusive equation has been thoroughly studied in a wide range of fields, particularly in dispersion problems. In early studies, the basic approach was to reduce the advection-diffusion equation to a purely diffusive problem by eliminating the advective terms. This was achieved via a moving coordinate system (e.g., Ogata and Banks, 1961; Harleman and Rumer, 1963; Bear, 1975; Guvanasen and Volker, 1983; Aral and Liao, 1996; Marshall et al.

or through the introduction of another dependent variable (e.g., Banks and Ali, 1964; Ogata, 1970; Lai and Jurinak, 1971; Marino, 1974; A
. To solve the equations, quite diverse mathematical methods are also employed, such as the Laplace transformation (McLachlan, 2014)
, the Hankel transform (Debnath and Bhatta, 2014), the Aris moment method (Merks et al., 2002), Green's function (Evans, 2010)
or superposition approaches (Lie and Scheffers, 1893) among others. More recent studies (e.g., Selvadurai, 2004) provide
time-dependent analytical solutions for which Darcy flow is applicable, yet it lacks an appropriate set of boundary conditions
given the infinite length of the domain.

~~Since then, dynamic 3D ice-sheet models have been used to investigate the mechanisms underlying HEs~~Steady-state ice temperature distribution studies also provide analytical solutions in bounded spatial domains, but fall short if the transient nature of the solution is to be captured. This is the case of the studies on the shear heating margins of West Antarctic ice streams (e.g., Perol and Rice, 2011, 2015) for which a steady but more refined one-dimensional thermal model was produced, first introduced by Zotikov (1986). Meyer and Minchew (2018) later solved a similar advective-diffusive problem under stationary conditions accounting for a constant strain-heating rate and further neglecting lateral (horizontal) advection after a scaling analysis. These one-dimensional studies imposed a stationary nature of the temperature distribution, thus assuming an idealised equilibrated energy state.

Despite these simplifications, heat transfer is well-known to be a three-dimensional process with a higher level of complexity that encompasses several mechanisms such as horizontal and vertical advection, the potential presence of liquid water within the ice, a varying ice thickness, internal heat deformation and frictional heat production among others (Greve and Blatter, 2009). Full numerical models are therefore also essential if a simultaneous consideration of such mechanisms needs to be achieved (Winkelmann et al., 2011; Pattyn, 2017).

Numerical models require caution as their accuracy and consistency must be previously assessed. Intercomparison projects are thus fundamental since they can provide consensus in a series of benchmark experiments that further serve as a reference solution for validation. In this context, analytical descriptions are extremely useful as they provide a control irrespective of the resolution or discretization schemes. For instance, ~~Marshall and Clarke (1997) used a 3D model to simulate the LIS, though no discharges were reproduced within the wide range of model parameters. **?** first modeled oscillatory behaviour in three-dimensional Shallow Ice Approximation (SIA) models with *ad hoc* basal sliding. Along with other studies, the authors noted the necessary evolving drainage and till mechanics providing potential insight into our understanding of~~ the ~~physical processes that caused Hudson Strait oscillations (**?**, **?**; 2010) . From highly reduced models (e.g. , Tulaczyk et al., 2000b) to a complex Herterich-Blatter-Pattyn ice model (e.g., Bougamont et al., 2011), multiple approaches have been found for a wide degree of comprehensiveness in ice stream dynamics in which the basal hydrology has become essential for an appropriate representation of~~ authors of the ~~ice streams~~EISMINT benchmarks, Huybrechts and Payne (1996), already noted the lack of analytical temperature solutions for such cases. Previously obtained solutions relied on strong assumptions regarding the particular vertical velocity profile (linear profile, Robin 1955; quadratic, Raymond 1983) and therefore an independent analytical description of the temperatures was not available.

There is an inevitable compromise when designing models that are both mathematically solvable and capable of accurately representing real-world phenomena. It is thus of utmost importance to carefully navigate this trade-off, deciding the appropriate

level of analytical tractability and physical realism based on the specific goals of the study. Attaining the right balance allows for meaningful insights while avoiding excessive computational demands or oversimplification that may hinder accurate representation and understanding of the real-world system.

~~More recently, Robel et al. (2013) focused on the temporal variability of an ice stream accounting for basal hydrology, modeled as a single lumped spatial element assuming a single velocity to represent ice discharge. The surface temperature and the~~ Simplified solutions, or those with reduced dimensionality are however useful. In this line, Dahl-Jensen et al. (1998) inferred past climatic and environmental conditions via a thermodynamic ice-core analysis using a one-dimensional numerical model. Their study relied on assumptions regarding the stationary behaviour of ice columns during the core formation process. The temperature history was divided in 125 intervals where the Monte Carlo method tests randomly selected combinations of surface temperatures and geothermal heat flux ~~were found to be important controls of the character of the ice flow. In particular, an oscillatory binge-purge mode was also present and appeared to be primarily caused by re-freezing of meltwater due to ice thinning during stagnation. The remarkable dependence of both the periodicity and the amplitude of these events on the boundary conditions of the system (surfacetemperature and geothermal heat flux) suggests that even a zero-dimensional spatial model (i.e., a single spatial element) is highly sensitive to time-independent forcing.~~

~~Nevertheless, none of these studies discussed the theoretical implications of estimating HE periodicity under the assumption of a (oversimplified) semi-infinite domain.In addition, these assumptions lack a more general treatment of the plausible boundary conditions at the top of the ice column. Despite the fact that the characteristic binge timescale determined the HE periodicity solely from environmental factors (lapse rate and sea level temperature) in prior studies, it does not necessarily imply that such periodicity is independent of the atmospheric temperature conditions and the energy balance across the ice-air interface . Strictly speaking, one can only conclude that the periodicity T cannot be imposed by a harmonic forcing at the~~ densities. Vertical profiles were compared to numerically-obtained profiles assuming an unchanged surface temperature.

Other numerical studies have incorporated more realistic transient behaviour, while often relying on diverse simplifications. For instance, Robel et al. (2013) assumed a linear vertical temperature profile to simplify the calculation of vertical heat conduction within an ice stream. While this simplification facilitated the analysis, it limited the accuracy and realism of their temperature solutions. A linear profile further implied an equilibrated energy state and an instantaneous perturbation of basal temperatures for a given surface temperature variation.

Traditional approaches both from numerical and analytical perspectives assume the simplest heat-flux boundary condition at the ice surface: the imposition of the air temperature at the uppermost ice layer. Nevertheless, in view of the surface fraction of the Greenland and Antarctic Ice Sheets covered by a firn layer (90% and ∼100%, respectively, Noël et al., 2022; Brooke et al., 2022), a more sophisticated description of the energy balance between the ice and the atmosphere may be beneficial. Already noted by Carslaw and Jaeger (1988), prescribing a fixed temperature is in fact a limit case of a broader set of boundary conditions known as 'linear heat transfer' or 'Newton's law of cooling' that accounts for a more realistic heat flux across the interface given by the temperature difference between the two media.

~~Even so,~~ In this study, we analytically solve the time-dependent problem of an advective-diffusive ice column in the presence of strain heating with a sophisticated surface boundary condition (Robin type, e.g., Gustafson and Abe, 1998). Our approach

accounts for the temporal evolution of the ~~$T \approx 7000$ year periodicity appears widely used in the literature as a reference value for ice-sheet models. Yet the theoretical implications of treating the problem with a more realistic finite medium remain unexplored. We herein investigate the consequences of considering a one-dimensional motionless ice column with a finite thickness L and quantify the impact of explicit boundary and initial conditions . A~~ temperature distribution rather than assuming an equilibrated state, thus allowing for a more accurate representation of the ice behaviour in response to changing external conditions. By considering time-dependent processes, we aim to improve the understanding of ice dynamics, particularly in scenarios where glacier and ice sheet response to climate change is a key concern. Moreover, transient solutions offer the potential to refine the interpretation of ice core data, leading to improved reconstructions of past climatic conditions and additionally provide analytical solutions to the time-dependent temperature profile problem that can constitute a helpful benchmark to numerical thermomechanical models of ice sheets. The formulation of the problem considered here is given in Section 2; the approach followed in this work is presented in Section 3; analytical solutions are shown in Section 4; results are discussed in Sections 5, 6 and 7; our concluding remarks are given in Section 8.

2 ~~Finite thickness~~Advective-diffusive ice column

Let us now elaborate on the physical description of a more realistic one-dimensional ice column with ~~a finite thickness L~~diffusive heat transport, vertical advection and strain heat. Our domain is ~~then~~ defined as the interval ~~$y \in [0, L] \equiv \mathcal{L}$. First, we must reformulate~~ $z \in [0, L] \equiv \mathcal{L}$. We shall formulate the problem imposing ~~the necessary additional~~ a generalized boundary condition at the top of the ~~motionless column $y = L$~~ column, $z = L$ (Fig. 1).

In the simplest physical scenario, the ice surface temperature is set to the air temperature value $\theta(L, t) = T_{\text{air}}$. However, the particular surface temperature is in fact the result of the energy balance between the ice and the atmosphere. ~~A more general approach considers that the ice and the air may not be always at thermal equilibrium, thus yielding a heat flux due to a vertical temperature gradient. The thermal equilibrium is only reached if the ice surface and the atmosphere temperatures are identical. In such conditions , the heat flux across the interface is null and the vertical gradient at the top~~ To address this limitation, we refine the surface boundary condition by incorporating a potential deviation from the air temperature, accounting for the insulation effect given by a firn layer in the uppermost region of the ice column. This is a highly probable scenario considering as explained in Section 1. The thermal insulation effect is a direct consequence of the firn density reduction towards the surface (e.g. Stevens et al., 2020) and falls within the so-called linear heat-transfer boundary conditions or 'Newton's law of Cooling' (Carlsaw and Jaeger, 1989, Chapter § 1.9).

This refinement enables a more accurate representation of the surface heat transfer dynamics and contributes to a comprehensive understanding of the energy balance within the ice column~~vanishes~~. In this description, both the surface ice temperature ~~and the vertical gradient can consequently~~ $\theta(L, t)$ and its vertical gradient $\theta_z(L, t)$ can vary in time:

$$\beta\theta_{yz} + \theta = T_{\text{air}}, \quad yz = L, \; t > 0, \tag{1}$$

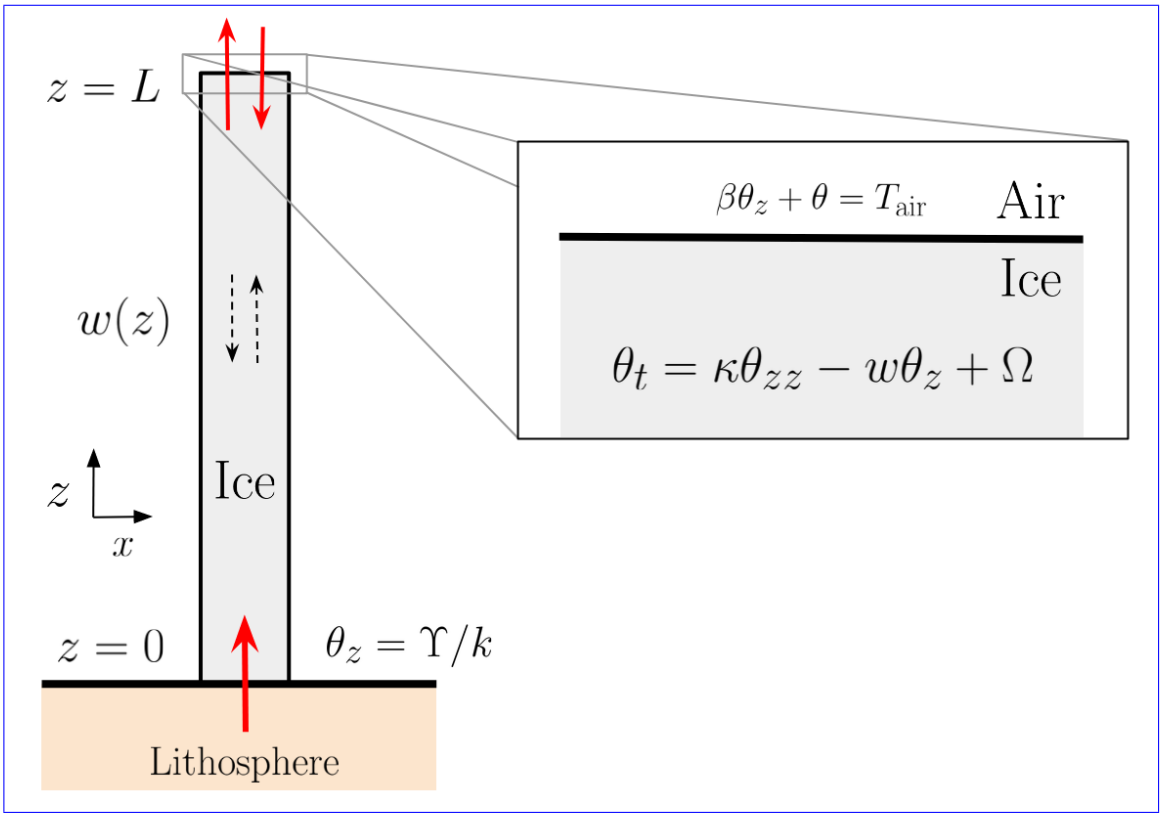

Figure 1. Schematic view of the ~~motionless~~ one-dimensional ice column with ~~a finite thickness L~~vertical advection $w(z)$ and strain heat source term Ω. Temperature evolution is dictated by the heat equation and an appropriate set of initial and boundary conditions. Subscripts denote partial differentiation. At the top, both the ice temperature and the vertical gradient can vary in time, thus allowing for non-equilibrium thermal states across the ice-air interface. At the base, the vertical gradient is fixed to the value given by the combined contribution of geothermal heat ~~flux $\theta_z = -G/k$~~flow and potential basal frictional heat $\theta_z = -\Upsilon/k$. Note that our formulation is one-dimensional so that the x-axis is solely introduced for visualization.

where italic subscripts denote partial differentiation and β is a parameter with length dimensions that modulates the permissible deviation between ice and air temperatures ~~. Equation ?? falls within the so-called linear heat transfer boundary conditions (e.g., Carslaw and Jaeger, 1988, Chapter § 1.9) and β~~ and is often referred to as the surface thermal resistance (per unit area).

This refined boundary condition reflects the fact that the ice and the air may not be always at thermal equilibrium, and allows for a heat flux due to a vertical temperature gradient. The thermal equilibrium is only reached if the ice surface and the atmosphere temperatures are identical. In such conditions, the heat flux across the interface is null and the vertical gradient at the top the ice column vanishes regardless of the value of β.

We can then physically interpret ~~this parameter~~ β as the thermal insulation of the ice-air interface. In other words, β is a length-scale over which the ice column feels the air temperature. A zero value corresponds to an ideal conductor ~~($~~$\theta(L,t) =$

T_{air}), whereas $\beta \to \infty$ represents a perfect thermal insulator characterized by a null heat exchange across the interface. In the limit case $\beta = 0$, the interface ice-air is always at thermal equilibrium (i.e., $\theta = T_{\text{air}}$). For $\beta \neq 0$, we allow for a heat exchange across the ice surface driven by the temperature difference between the two media.

Considering diffusive heat transport, vertical advection, and a potential heat source, the ice temperature $\theta(y,t)$ $\theta(z,t)$ satisfies an initial value problem given by the heat equation:

$$\begin{cases} \theta_t = \kappa\theta_{zz} - w\theta_z + \Omega, & \xi \in \mathcal{L},\ t > 0, \\ \theta = \theta_0(z), & z \in \mathcal{L},\ t = 0, \\ \theta_z = -\Upsilon/k, & z = 0,\ t > 0, \\ \beta\theta_z + \theta = T_{\text{air}}, & z = L,\ t > 0, \end{cases} \tag{2}$$

where G is the the heat source Ω is an inhomogeneous term that captures strain heat and horizontal advection, $\Upsilon = G + Q$ is the combined contribution of geothermal heat flux G and potential basal frictional heat Q, k is the ice conductivity and κ is the ice diffusivity(, assumed to be constantsince we do not explicitly consider the firn layer above the ice). We further consider a z-dependent vertical velocity component given by $w(z)$.

The initial temperature profile reads $\theta_0(y) = \theta_{\text{b}} + (\theta_{\text{L}} - \theta_{\text{b}})\, y/L$, where θ_{L} and θ_{b} are the initial temperatures at the top and the base of the column, respectively. This linear profile is introduced for simplicity and it allows us to explicitly determine the impact of the initial basalIn order to solve the problem, we must first provide the particular form of the vertical velocity term. As in Clarke et al. (1977) and Zotikov (1986), we first assume a linear variation of $w(z)$ with depth:

$$w(z) = w_0 \frac{z}{L} \tag{3}$$

where w_0 is the vertical velocity at the ice surface $z = L$. This dependency is widely used in the literature (e.g., Joughin et al., 2002, 2004; S and standard values for w_0 usually read 0.1-0.2 m/surface ice temperature independently. yr (Glovinetto and Zwally, 2000; Spikes et al., 20 . Nonetheless, we will further explore in Section 6 a more general relationship that better describes vertical velocities modeled by Glen's flow law as discussed in the EISMINT benchmark experiments (Huybrechts and Payne, 1996).

We must stress that the system described as above (Eq. 2) builds upon MacAyeal (1993a) and aims at a purely vertical diffusive heat-transfer description of a motionless ice column. In reality, heat transfer is well-known to be a three-dimensional process with a higher level of complexity that encompasses several mechanisms as horizontal/vertical advection , potential presence of liquid water within the ice, a varying ice thickness, internal heat deformation and frictional heat production among others. The current problem is approached by using analytical techniques and so the complexity of The inhomogeneous term Ω can encompass a number of processes, though here we focus on strain heating $\mathcal{S}$ and horizontal advection $\mathcal{H}$, so that $\Omega = \mathcal{S} + \mathcal{H}$. The strain-heating term $\mathcal{S}$ is a function of the system is critical if an analytical solution is to be found. The simplicity of our description provides new insight from a theoretical perspectivesecond invariant of the stress tensor. In general, it can be expressed as $\mathcal{S} = \sigma_{ij}\dot{\epsilon}_{ij}$, wherein σ_{ij} is the Cauchy stress tensor and $\dot{\epsilon}_{ij}$ is the strain rate tensor (expressed in index

notation). Applying Glen's law, the rate of strain heating can be simplified as:

$$\mathcal{S} = \sigma_{ij}\dot{\epsilon}_{ij} \simeq 2A^{-1/n}\,\dot{\epsilon}_{\text{lat}}^{(n+1)/n} \tag{4}$$

where $\dot{\epsilon}_{\text{lat}} = \dot{\epsilon}_{12} = u_x/2$ assumes that the dominant component of the strain rate tensor is the lateral strain rate $\dot{\epsilon}_{\text{lat}}$ (e.g., Meyer et al., 2019) and summation is implied over repeated indexes. This assumption ensures the analytical tractability of the solution while including a potential constant strain contribution throughout the ice column.

3 ~~Fourier method~~

~~Our aim is to solve the initial boundary value problem by using the Fourier method, also known as separation of variables (an overview of the method is given in Appendix A, for a standard reference see e.g., Kalnins et al., 2018). Consequently, we first need to find a change of variable that leaves us with homogeneous boundary conditions in order to determine the corresponding eigenvalues~~The horizontal advection term $\mathcal{H}$ can imply a heat source or a sink depending on the sign of the horizontal temperature gradient along a particular direction. We herein consider such a contribution by defining a depth-averaged lateral advection term (Meyer et al., 2019):

$$\mathcal{H} = \int_0^1 (\mathbf{u}\cdot\hat{\mathbf{n}})\,\theta_{\hat{\mathbf{n}}}\,d\xi, \tag{5}$$

where $\mathbf{u}$ is horizontal velocity vector, $\hat{\mathbf{n}}$ is the normal vector along an arbitrary direction contained in the horizontal plane and $\theta_{\hat{\mathbf{n}}} = \partial\theta/\partial\hat{\mathbf{n}}$ denotes the directional derivative along $\hat{\mathbf{n}}$.

~~Let us then define the new variable $\xi(y,t)$ for the problem determined by~~ This assumptions allow us to include a potential strain heat source $\mathcal{S}$ and a horizontal advection of heat term $\mathcal{H}$ while keeping the analytical tractability of Eq. 2~~:~~

$$\xi = \theta - T_{\text{air}} + (y - \beta - L)\,\frac{G}{k}$$

~~Therefore, in terms of the new variable the problem under consideration reads:~~ . The limitations of these simplifications are discussed in Section 7.

$$\begin{cases} \xi_t = \kappa\xi_{yy}, & y \in \mathcal{L},\ t > 0, \\ \xi = f(y), & y \in \mathcal{L},\ t = 0, \\ \xi_y = 0, & y = 0,\ t > 0, \\ \beta\xi_y + \xi = 0, & y = L,\ t > 0, \end{cases}$$

~~where the initial state is $f(y) = \theta_0(y) - T_{\text{air}} + (y - \beta - L)\,\frac{G}{k}$.~~

3 Analytical solution

~~As a result, we now have a homogeneous problem that can be solved by~~ Let us outline our analytical approach. We first non-dimensionalise our problem and exploit the linearity of the differential operator by further decomposing the solution as a sum of stationary and transient components to deal with the inhomogeneity. Lastly, we apply separation of variables ~~(Appendix A). If a solution exists, it determines the vertical temperature profile at any given time for the~~ to obtain a solution of the time-dependent problem and impose the corresponding initial and boundary conditions~~provided by Eq. 2~~. Derivation details are elaborated in Appendix A.

4 ~~Analytical solution~~

~~The solution $\xi(y,t)$ to the boundary problem determined by the Set 2 (derivation details in Appendix B) reads:~~

It is natural to non-dimensionalise our problem by defining the following variables:

$$\xi(y=\frac{z}{L},\ \tau=\frac{\kappa}{L^2}t),\ \theta=\sum_{n=0}^{\infty}A_n\cos\sqrt{\lambda_n}ye^{-\kappa\lambda_n t}\frac{T}{T_{\text{air}}},\ \tilde{w}=\frac{L}{\kappa}w,\ \tilde{\beta}=\frac{\beta}{L},\ \tilde{\Omega}=\frac{L^2}{\kappa T_{\text{air}}}\Omega \tag{6}$$

where ~~the eigenvalues λ_n are given by the transcendental equation:~~

$$\cot\left(L\sqrt{\lambda_n}\right)=\beta\sqrt{\lambda_n}.$$

~~Equation ?? does not admit an algebraic representation, hence requiring a numerical method to compute λ_n. Here we implemented the Brent-Dekker algorithm (Dekker, 1969; Brent, 1971) with a tolerance of 10^{-8}. This root-finding algorithm choice combines the bisection method, the secant method and the inverse quadratic interpolation.~~

~~The coefficients A_n can be readily obtained applying orthogonality among eigenfunctions:~~ tildes are hereinafter dropped to lighten the notation.

$$A_n=\frac{2}{L}\int_0^L\xi(y,0)\cos\left(\sqrt{\lambda_n}y\right)dy.$$

Hence, we can express our Problem 2 as:

$$\begin{cases}\theta_\tau=\theta_{\xi\xi}-w\theta_\xi+\Omega, & \xi\in\tilde{\mathcal{L}},\ \tau>0,\\ \theta=\theta_0(\xi), & \xi\in\tilde{\mathcal{L}},\ \tau=0,\\ \theta_\xi=\gamma, & \xi=0,\ \tau>0,\\ \beta\theta_\xi+\theta=1, & \xi=1,\ \tau>0,\end{cases} \tag{7}$$

It is noteworthy that if β is strictly zero where $\gamma = -T_{\text{air}}\Upsilon/(kL)$, $w = \text{Pe}\,\xi$ and $\theta_0(\xi)$ are the non-dimensional geothermal heat flux, vertical velocity and initial profile respectively. The vertical velocity has thereby been conveniently expressed in terms of the Peclét number $\text{Pe} = w_0 L/\kappa$ (i.e., the ice surface temperature is prescribed $\theta(L,t) = T_{\text{air}}$), the solution is equivalent to finding the eigenvalues satisfying the equation $\cos\left(L\sqrt{\lambda_n}\right) = 0$ and can be obtained analytically as :

$$\sqrt{\lambda_n} = \left(n + \frac{1}{2}\right)\frac{\pi}{L},$$

where $n = 0, 1, 2, \ldots$ ratio of advective to diffusive heat transport). The non-dimensional strain heat source term $\mathcal{S}$ can be identified with the Brinkman number Br as noted in Table 1, which represents the ratio of deformation heating to thermal conduction (see Table 2).

In this particular case, the corresponding coefficients A_n also allow for analytical expression:

$$A_n = 4(\theta_{\text{b}} - \theta_{\text{L}})\left[\frac{\cos(n\pi)}{2n\pi + \pi}\right] - 8L\frac{\tilde{G}}{k}\left[\frac{1}{2n\pi + \pi}\right]^2.$$

Employed parameter values and range further explored in Fig **??**. **Magnitude** **Symbol** **Fixed value** **MacAyeal (1993)** **Explored range** (units)(Fig. **??**) Initial ice basal temperature θ_{b} $(^\circ C)$ -10.0 -10.0 -50,-10Initial ice surface temperature θ_{L} $(^\circ C)$ -25.0 N/A -50,-10Geothermal heat flux G (mW/m^2) 50.0 32.0 25,100Air temperature T_{air} $(^\circ C)$ -25.0 N/A -50, -10

4 Vertical temperature profile

We now present the vertical profiles $\theta(y,t)$ from analytical solutions given by Eq. **??** for three different thicknesses, The non-dimensional number γ is the combined contribution of geothermal heat flux and potential basal frictional heat, normalised by the vertical temperature gradient that would exists for a column thickness L = 1.0and temperature T_{air}. It provides the relative strength of the basal inflow of heat compared to the ice-column extent and the air temperature.

The dimensionless problem clearly shows that four numbers completely determine the shape of the stationary solution: γ, 1.5 and 2.5 km, at $t = 0$ β, Pe and $t = 4750$ years (Fig. **??**) using the set of paramters described in Table **??**. The second time frame value is chosen so that the fastest warming scenario (blue line Br. Their particular impact on the temperature distributions is shown in Fig. **??**) precisely reaches melting. Since solutions are presented as infinite series, truncation was naturally required. We kept 100 terms in Eq. **??**, though the error is below 0.03% after the 13th term. 2.

The implications of a finite domain are quite notable. Particularly, the column base warms due to the geothermal heat flux at a rate that is proportional to $\sim \kappa\lambda_0 e^{-\kappa\lambda_0 t}$ at leading order. Then if we let $L > \tilde{L}$ be two thicknesses, it consequently yields that the ratio $\theta_t/\tilde{\theta}_t \sim e^{-\kappa(\lambda_0 - \tilde{\lambda}_0)t}$ exponentially growsGiven that Eq. 7 is inhomogeneous, we will decompose the solution as a sum of a transient $\mu(\xi,\tau)$ and a stationary $\vartheta(\xi)$ components, so that rate of change (at $y = 0$) is larger for a thicker column since the corresponding eigenvalues $\lambda_0 < \tilde{\lambda}_0$. That is, a thicker ice column implies a faster change of its basal temperature$\theta(\xi,\tau) = \mu(\xi,\tau) + \vartheta(\xi)$. As a result, the transient and stationary problems are subject to homogeneous and

inhomogeneous boundary conditions respectively:

$$\begin{cases} \mu_\tau = \mu_{\xi\xi} - w\mu_\xi, & \xi \in \tilde{\mathcal{L}},\ \tau > 0, \\ \mu = \mu_0, & \xi \in \tilde{\mathcal{L}},\ \tau = 0, \\ \mu_\xi = 0, & \xi = 0,\ \tau > 0, \\ \beta\mu_\xi + \mu = 0, & \xi = 1,\ \tau > 0, \end{cases} \tag{8}$$

and

$$\begin{cases} \Omega = \vartheta_{\xi\xi} - w\vartheta_\xi, & \xi \in \tilde{\mathcal{L}}, \\ \vartheta_\xi = \gamma, & \xi = 0, \\ \beta\vartheta_\xi + \vartheta = 1, & \xi = 1, \end{cases} \tag{9}$$

where $\mu_0 = \theta_0(\xi) - \vartheta(\xi)$ in the initial profile of the transitory solution.

The ~~impact of β is particularly clear at the top (Fig. **??**) , where the temperature slightly increases due to an upward heat flux originating at the base (unlike the $\beta = 0$ case, where the temperature is prescribed) . We have chosen $\beta = 100$ m to display such mechanism, whilst keeping a reasonable temperature difference (Kurt M. Cuffey, 2010).~~

~~Initial temperature profile. Temperature profile after 4750 years. Vertical profiles from analytical solutions $\theta(y,t)$ for three different ice-column thicknesses $L = 1.0$, 1.5, and 2.5 km. Left panel (a), $t = 0$ yr; right (b), $t = 4750$ yr. Solid line represents solutions for $\beta = 100$ m where the case $\beta = 0$ is denoted by a dotted line. Parameter values employed are shown in Table **??** (fixed value column)~~

~~Figure **??** further focuses on the basal temperature evolution by comparing the effects of a particular zero/non-zero β value for different ice thicknesses, yet it does not provide information about the relevance of the particular β choice. The implications of this choice and their relative magnitude compared to the total thickness is thoroughly presented in Figs. **??** and **??**. Since this thermal insulator parameter has length dimensions, it is illustrative to study its dependency referred to the particular column thickness L,~~ solution to the stationary component (Eq. 9) already differs from previous analytical works as Robin (1955) and Lliboutry (1963). First, they considered a homogeneous version of the problem (i.e., ~~the dimensionless quantity β/L shown in Fig. **??**. As β becomes small compared to the ice thickness~~ $\Omega = 0$) so that potential strain heating or horizontal advective contributions are neglected. Moreover, they simplified the top boundary condition $\xi = 1$ since they imposed a prescribed constant temperature value (see also Clarke et al., 1977). However, these refinements still allow for analytically tractability and thus the stationary solution is (see Appendix B for derivation details):

$$\vartheta(\xi) = \Omega\frac{\xi^2}{2}\,{}_2F_2\left(1,1;\frac{3}{2},2;-\zeta\right) + A\,\mathrm{erf}\,[a\xi] + B \tag{10}$$

where ${}_2F_2(a_1,a_2;b_1,b_2,x)$ is the generalised hypergeometric function, $\zeta = (a\xi)^2$, $a = (w_0/2)^{1/2}$, $A = -\gamma(\pi/(4a))^{1/2}$ and $B = 1 - A\left(2a\pi^{-1}\beta e^{-a^2} + \mathrm{erf}\,[a]\right)$. Note that if the inhomogeneous term is zero (i.e., ~~$\beta/L \ll 1$~~$\Omega = 0$), the ~~ice surface remains~~

cold by the influence of the atmosphere temperature ($T_{\text{air}} = -25\,^{\circ}\text{C}$). The entire profile is affected by the surface condition and thus the basal temperature remains lower as well. On the contrary, if we let $\beta/L = \mathcal{O}(1)$, we find that the ice surface monotonically warms (due to the upwards geothermal heat flux and the imposed larger insulating condition)and the base reaches melting faster. This behaviour yields two points worth noting: (1) the saturation in basal temperature for $\beta/L > 0.5$ and (2)a "never-thawing" base for sufficiently low β/L values. stationary temperature profile reduces to the well-known error function previously obtained by Robin (1955) and Lliboutry (1963). Even so, the temperature distribution would still differ as the boundary condition considered herein reflects a potential insulating top layer unlike prior studies.

To complete our study on the impact of the particular β/L choice, we represent the ice surface temperature deviation from the air temperature boundary condition normalised by the latter as $\Delta\theta = (\theta(L) - T_{\text{air}})/T_{\text{air}}$ (blue solid line, Fig. **??**). We thus obtain a dimensionless quantity that reflects the surface temperature changes as a function of the relative thermal insulation referred to the column thickness. The particular ice surface temperature is evaluated when the base reaches melting (red solid line, Fig. **??**)so as to ensure that the incoming energy is entirely diffused and there are no phase changes. We find ice temperature deviations up to a 30% from the air temperature (imposed as a boundary condition) in We now take a step further and allow for time evolution by solving Eq. 8 and building our solution as the sum of both contributions. Namely, the limit $\beta/L \to 1$general solution of the transient problem $\mu(\xi,\tau)$ is (see Appendix A for derivation details):

$$\mu(\xi,\tau) = \sum_{n=0}^{\infty} \left[A_n \Phi\left(\alpha_n;\delta;\zeta\right) + B_n \Psi(\alpha_n;\delta;\zeta)\right] e^{-\lambda_n \tau} \tag{11}$$

where $\Phi\left(\alpha;\delta;\zeta\right)$ and $\Psi\left(\alpha;\delta;\zeta\right)$ are the Kummer (Kummer, 1836) and Tricomi confluent hypergeometric functions respectively (also known as confluent hypergeometric functions of the first and second kind). $\alpha_n = -\lambda_n/(2w_0)$ and $\delta = 1/2$. As the solution must be bounded at the origin, we set $B_n = 0$.

Time evolution of the basal temperature for three different thicknesses (in km). Solid line represents solutions for $\beta = 100$ m whereas the limit case $\beta = 0$ (i.e., fixed surface temperature) is denoted by a dotted line. The boundary condition at the base is identical for all cases and given by the geothermal heat flux G. The horizontal dashed lines represent the corrected pressure melting point for each column thickness. The full solution $\theta(\xi,\tau) = \vartheta(\xi) + \mu(\xi,\tau)$ thus reads:

$$\theta(\xi,\tau) = \Omega\frac{\xi^2}{2}\,{}_2F_2\left(1,1;\frac{3}{2},2;-\zeta\right) + A\,\text{erf}\left[a\xi\right] + B + \sum_{n=0}^{\infty} A_n \Phi\left(\alpha_n;\delta;\zeta\right) e^{-\lambda_n \tau} \tag{12}$$

where the coefficients A_n are obtained from the initial temperature profile (Eq. A.2 in Appendix A).

4 ~~A new period for the binge/purge oscillator~~

4 Stationary solutions

Prior to a detailed discussion of our results, we must note that the solution to our Robin boundary problem (Eqs. **??** - **??**)describes the evolution of Before displaying the results of the full time-dependent problem, it is worth noting that the

~~temperature profile only until the ice column base thaws, and therefore does not show a periodic behaviour of the ice dynamics. Such behaviour emerges once this solution is considered within MacAyeal's oscillator (MacAyeal, 1993a, b).~~ consideration of a more sophisticated energy exchange at the ice-air interface entails a perturbation in the entire temperature distribution.

~~The temporal dependency of the basal temperature (Fig.??) from our analytical solution (Eq.??)allows us to calculate the time required for the column base to reach the melting point analogously to the growth phase of a Heinrich event oscillation (MacAyeal, 1993a). We also account for the pressure correction of the ice melting point as $\theta = \tilde{\theta} + \alpha P$, where $\alpha = 9.8 \cdot 10^{-8}$ K/Pa (e.g., Greve and Blatter, 2009). Knowing that $P = \rho g L$ and our column spans the following thickness interval $L = [1.0, 3.5]$.For $\Delta L \simeq 3.0$ km, then $\tilde{\theta} \simeq -2.6$ ºC yields a non-negligible correction, making the ice thickness dependence even stronger as a result of two independent contributions: a more significant insulating effect of a thicker ice columnand a larger pressure melting correction~~Figure 2 shows our steady-state solutions as vertical profiles for a subset of the permutations of the non-dimensional numbers Pe, Br, γ and β. It is illustrative to compare the shape of our temperature solutions with Clarke et al. (1977) (Fig. 1 therein). We must stress that a one-to-one comparison is not readily possible since they imposed a simpler top boundary condition in which the ice surface temperature is fixed to a given value, though the exact same solutions can be simply obtained by setting $\beta = 0$ in our case (see Eq. 1).

It is of utmost importance to consider the particular sign of the vertical advection term. In the positive case $w_0 > 0$ (i.e., ϑ^+), the geothermal heat flux travels upwards not solely by diffusion but also enhanced by the vertical transport, thus warming the entire column more efficiently and reaching a higher equilibrium temperature. On the contrary, in the negative case $w_0 < 0$ (i.e., ϑ^-), colder ice is advected from the uppermost part of the column, consequently cooling down the profile. It is worth ~~stressing that the period of the binge-purge oscillator (MacAyeal, 1993a) did not considered any pressure melting correction so that a one-to-one comparison must dismiss such effect (see Section ??)~~noting the difference in x-axis scales for each case, meaning that the basal temperature variation is several times larger for the upwards vertical advection scenario.

~~Basal temperature. Surface temperature. Ice temperature time series for (a) Base and (b) Surface. Each line represents a particular dimensionless β/L choice. The strictly zero case corresponds to $\beta = 0$ and $L = 1.0$ km. A solid black lines denotes the semi-inifinite domain solution (Carslaw and Jaeger, 1988). The air temperature is fixed for all cases and reads $T_{\text{air}} = -25$ °C.~~

~~Normalised ice surface temperature deviation $\Delta\theta$ (dark blue line) from the air temperature boundary condition T_{air} and time required for the base to thaw (red line) as a function of the normalised insulating parameter β/L. The ice surface temperature deviation is evaluated when the base reaches melting.~~

~~Figure ?? shows the sensitivity of~~ The non-dimensionalization of our analytical model provides simplicity and further reduces the parameter dimensionality of the solutions to solely four numbers, each corresponding to one column in Fig. 2. The Peclét number produces the largest changes in the equilibrium solutions, with the well-known linear profile resulting for the ~~thermal state of the base to the thickness of the column L and to the treatment of the surface boundary condition. It is clear that the column thickness is a fundamental factor that allows the surface temperature to influence the evolution of the base. Strictly speaking, the external forcing perturbs the temperature vertical profile of the ice column, thus determining the basal temperature. When we allow for non-equilibrium thermal states in the top boundary condition~~ purely diffusive case

(i.e., ~~$\beta \neq 0$~~)$\mathrm{Pe} \to 0$). The normalized geothermal heat flux also yields large temperature amplitudes within the explored range. Nevertheless, for $w_0 < 0$, the impact is clearly reduced to the lower half of the column, thus leaving the upper regions nearly unperturbed. An even more unique behaviour is also found for the ~~base warms faster since the columnsurface can evolve in time towards higher temperatures, thus inducing a lower temperature difference between the base and the top. The relevance of this effect is inversely proportional to the column thickness, becoming negligible for large L values.~~

~~When computing the time required for the base to thaw, the initial temperature profile plays an essential role. The linear profile is imposed as the initial condition of our analytical solution (Eq. **??**) and then, a broad range of θ_b~~ surface insulation β and the rate of strain heating Br in the presence of downwards advection, where the entire temperature profile is left unchanged despite varying values of β and ~~θ_L values is explored to quantify their impact on this timescale (Fig. **??**)~~ Br. This can be understood as the independence of the particular heat exchange at the ice-air interface if colder ice is transported downwards and a far more effective heat transport due to advection ($\mathrm{Pe} = 7$ in both cases) than dissipated through strain deformation.

5 Full solutions

We now present the results of the problem presented in Eq. 2 by considering a more realistic time-dependent description. This transient nature depends on the initial state of the system, although it exponentially converges to the stationary case as the transient component vanishes under the assumption of constant boundary conditions. ~~Ideally, the initial condition should be set by the temperature profile immediately after an event in the binge-purge cycle, yet such a profile is not available. A linear profile assumes that the temperature in the ice reflects a linear lapse rate in the atmosphere as the ice thickness builds up over time.~~

~~Figure **??** also shows the dependency of this basal-thawing timescale on the boundary conditionsin our general formulation (Eq. **??**). The impact of the external forcing is evident from Fig~~To illustrate the full solutions, we show the explicit time evolution from an initial profile as it approaches the corresponding stationary solution (Fig 3). In this instance, we employ a constant initial temperature profile for simplicity $\theta_0(\xi) = 1.5$. With this particular choice, we ensure that the full solution is below and above of the stationary solution for the upward and downward advection scenarios, respectively. We must stress a few points here. In Fig. 3a, the uppermost region of the ice column rapidly reduces its temperature due to the effect of a colder air temperature as the geothermal heat flux contribution requires a longer time to travel from the base. On the contrary, the lower part of the domain increases its temperature notwithstanding the sudden decrease of the upper half. Once the geothermal heat flux has propagated upwards, the ice surface temperature slowly starts to increase. This is possible since we are here solving for a non-zero β value that allows for a difference between the air and the ice surface temperatures. The rate of increasing temperature gradually diminishes and it approaches zero as the transient solution asymptotically reaches the temperature profile given by the stationary temperature profile $\vartheta(\xi) = \lim_{\tau \to \infty} \theta(\xi, \tau)$. ~~**??**. As we would expect, lower T_{air} values yield longer basal-thowing timescales, though solely for ice thicknesses below ~ 2 km. For thicker ice, the periodicity appears to be independent of the surface ice temperature. We therefore find that, for this parameter choice (Table **??**), $L_{\mathrm{thr}} = 2$ km is a~~

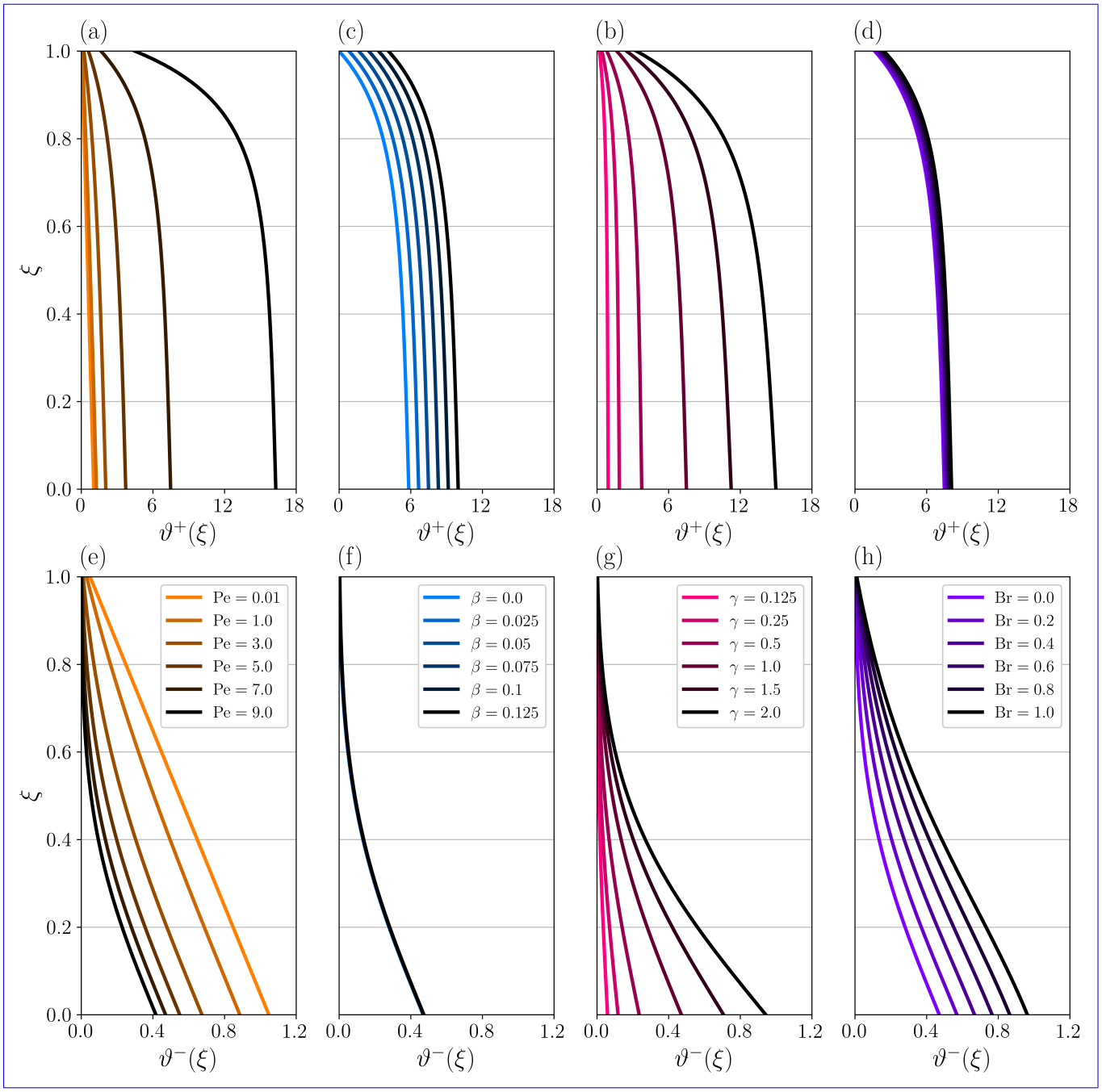

Figure 2. Stationary vertical non-dimensional temperature profiles $\vartheta(\xi,\tau)$. Upper row: upward vertical advection. Lower row: downward vertical advection. Note the different x- axis scale. Solutions are fully determined by four non-dimensional numbers: Pe, β, γ and Br, corresponding to each column respectively. The remaining three numbers are left unchanged in each column to allow for comparison. First column: $\gamma = 1.0$, $\beta = 0.05$. Second: $\gamma = 1.0$, Pe $= 7$. Third: $\beta = 0.05$, Pe $= 7$. Fourth: $\beta = 0.05$, Pe $= 7$, $\gamma = 1.0$. The Brikman number Pe is identically zero in all profiles but the fourth column.

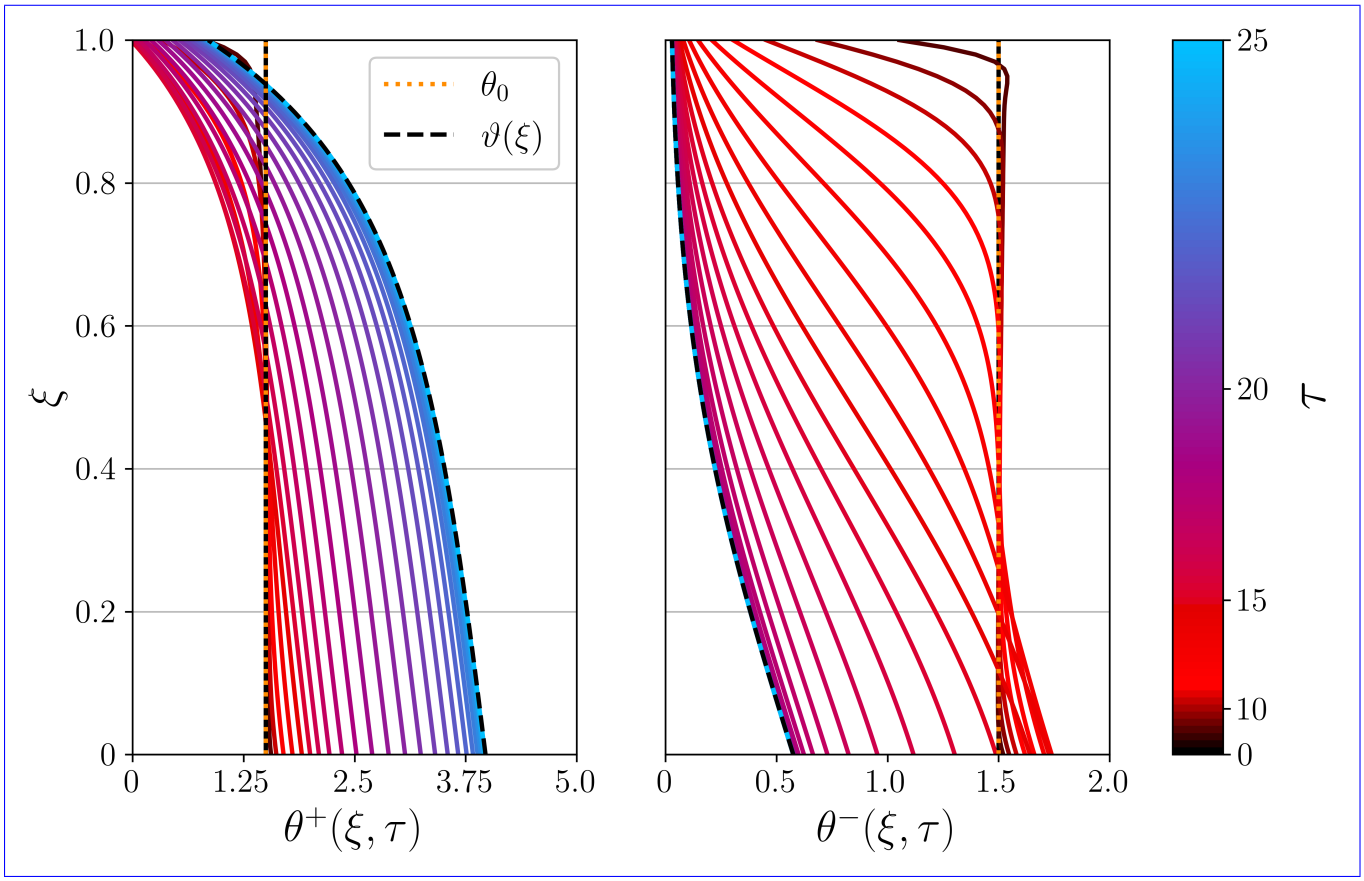

Figure 3. Time-dependent solution given an initial temperature profile $\theta_0(\xi)$ (vertical dotted line). For simplicity, we here assume $\theta_0(\xi) = 1.5$ to illustrate the time-scale differences between the upwards and downward advection scenarios denoted by θ^+ and θ^-, respectively. Dimensionless values: $\mathrm{Pe} = 5.0$, $\gamma = 1.0$, $\mathrm{Br} = 0.1$ and $\beta = 0.05$. Black dashed lines represent the stationary solutions $\vartheta(\xi)$. To ease visualization, the time variable is cubically spaced as indicated in the colourbar.

~~threshold value above which the time required to thaw is decoupled of the top boundary condition. A distinct parameter choice will alter this particular value, yet we expect this behaviour to remain present.~~

~~Such a threshold is a compelling result and deserves further elaboration. Since here we focus on the time required for the base to thaw, it is fundamental to consider the temperature gradient between the base and the top. The vertical temperature~~
425 ~~gradient must be supported by~~

A similar behaviour is found in Fig. 3b. In this case, the base rapidly increases its temperature unlike the ice surface, where it suddenly diminishes. Even though the geothermal heat flux ~~. If the surface is too cold, the heat provided by G may not be sufficient to support a large enough temperature difference (within the column) so that the base reaches the melting point. For a given choice of G, k and T_{air}, there exists a minimum ice thickness L_{min} that yields a temperature gradient that allows for~~

the base to thaw. For thinner columns, is identical in both scenarios, the additional contribution of advected colder ice from the surface renders a new equilibrium profile in which not only the upper region of the column is colder, but also the base in itself.

To examine closely the transient nature of the base always remains frozen. This further translates in a sudden increase in the basal-thawing timescale solutions, we present the temperature evolution of a given initial profile for a certain range of the non-dimensional parameters (Fig. **??**). Although the value of this threshold depends on the physical properties of the ice and the boundary conditions 4). This gives us information about the time-dependent effects of each parameter, unlike Fig. 2 that was restricted to equilibrium states. Addtionally, the continuous representation (i.e., ~~k, G and T_{air}~~), the mechanism still holds irrespective of the particular parameter choicecolourbar in Fig. 4), as opposed to a discrete number of vertical profiles as in Fig. 3, facilitates comparison among particular parameter choices.

The time required for the base to thaw decreases as the geothermal heat flux increases.A similar behaviour is found with increasing L due to the thermal insulating effect of the ice column, particularly for lowgeothermal heat flux values.This is consistent with what we expected, as a higher geothermal heat flux provides a larger amount of heat (per unit time)to the ice column. particular parameter values were selected so that there would be two scenarios for each number and hence four permutations: low/high advection (i.e., Pe) and low/high geothermal heat (i.e., γ). This setup allows us to separately determine the role played by each mechanism during the transient regime of the solution.

The initial conditions are also essential to quantify the time required for the ice base to thaw. We have considered a linear initial vertical profile $\theta_0(y) = \theta_{\mathrm{b}} + (\theta_{\mathrm{L}} - \theta_{\mathrm{b}})\, y/L$, so as to understand the explicit dependency of For a fixed γ value (γ=1.0), the initial surface temperature θ_{L} and the initial basal temperature θ_{b} independently strength of advection is only relevant in the upward scenario (Figs. **??** and **??**) . Namely, the impact of θ_{L} is determined by the column thickness, with a more acute dependence for low L values. This was expected as the vertical temperature gradient increases for a fixed temperature difference between base and top if the column thickness is reduced. A never-thawing base is plausible when such a vertical gradient surpasses the value given by 4a and 4c) and yields considerably longer equilibratum times. In contrast, the downward case is nearly independent of the particular advection strength and rapidly reaches thermal equilibrium. A different behaviour is found when fixing advection and varying the geothermal heat flux . Lastly, the time required to melt the base appears to be rather sensitive to the initial basal temperature, rapidly reaching values above 25 kyr for $\theta_{\mathrm{b}} < -40^{\circ}$C. γ. In such a case, both regimes ($w_0 < 0$ and $w_0 > 0$) are perturbed by γ (Figs. 4e-h). Even so, the uppermost region of the column remains colder, unlike the high upward advection scenario in which the ice surface eventually increases its temperature due to the combined effect of diffusion and advection fostered by a thermally insulated ice surface ($\beta = 0.05$).

Figure **??** particularly shows a non-monotonic behaviour of the basal-thawing timescale with respect to the ice thickness. To understand this behaviour there are several factors that must be considered simultaneously. It is illustrative to look at the vertical profiles shown in Fig. **??**. The fact that T is non-monotonic with L at $\theta_{\mathrm{b}} < -30^{\circ}$C is a consequence of two factors: the necessary energy budget to warm an ice column and the vertical temperature gradient. For a fixed temperature difference between the base and Moreover, Figs. 4b and 4g clearly illustrate two different time scales. A rapid decrease in temperature at the upper half of the column is a direct consequence of the top, the former increases with Lsurface boundary condition, given that the air temperature is colder than the underlying ice. Nevertheless, we observe a second and slower response by the

upward transport of heat. Diffusion and advection gradually warm the column as the heat source (the geothermal heat flux) is located at the base. It eventually reaches the upper region and, in the case of high advection (Fig. 4c), entailing an increase in ice surface temperature. We must stress that the latter result is only possible due to a more refined top boundary condition (Eq. 1). If advection is diminished (Figs. 4e and 4g) the lower half still warms due to diffusion as it is closer to the heat source for sufficiently large values of γ, whereas the ~~latter decreases with L.~~ ice surface remains colder since diffusion is spatially limited.

~~For slight variations of the thickness δL around $L = 1.5$ km, while fixing the initial basal temperatureto e. g., $\theta_b = -30°C$, the time required to thaw the base increases regardless of the sign of δL. In other words, it takes longer~~

As shown by the colour legend in Fig. 3, the time required to reach the ~~melting point either for a thinner or a thicker column. This local minimum is a balance between the total energy necessary to heat the column and the fact that a thinner one implies a larger vertical gradient for a fixed~~ stationary state is considerably shorter for $w_0 < 0$. This is a consequence of the temperature difference between the ~~base and the top. If we consider the effect of these factors explicitly: first, a thinner column requires a smaller amount of energy to increase the temperature of~~ initial $\theta_0(\xi)$ and the stationary profile $\vartheta(\xi)$. It can be visualised by the enclosed area between the two curves: $\theta_0(\xi)$ and $\vartheta(\xi)$. Physically, this area represents the necessary energy Q for the initial state $\theta_0(\xi)$ to reach the equilibrium profile $\vartheta(\xi)$ so that $Q = \int_0^1 \Delta\theta(\xi)d\xi$, wherein $\Delta\theta(\xi) = \vartheta(\xi) - \theta_0(\xi)$. The sign of Q thus indicates the direction of the energy exchange, positive values meaning an increased thermal energy of the column.

More generally, we can also study the evolution of the energy content within the column by performing such an integration over the full solution $Q(\tau) = \int_0^1 \theta(\xi, \tau)d\xi$. This yields the corresponding energy content time series and provides information about the overall inflow or outflow of heat, irrespective of the local changes that the temperature profile might undergo (Fig. 5). Thus, from an arbitrary initial state, we can study how the total energy balance of the ~~column; however, considering the second factor, a thinner column would yield a larger vertical temperature gradient (ultimately yielding a slowdown in the warming rate as the geothermal heatflux is fixed in the BC). The combination of both effects allows for the local minima found in Fig. **??**~~ice column depends on the four dimensionless numbers that determine the stationary solutions (Fig. 2).

6 ~~The limit $L \to \infty$~~EISMINT

After studying the behaviour of the solutions both at the transitory and stationary regimes, we narrow down our focus to a particular case: the EISMINT benchmark experiments (Huybrechts and Payne, 1996). We can thus evaluate the non-dimensional parameters (Table 2) that determine our stationary solution and additionally re-dimensionalise the temperature profiles so as to ease a physical interpretation.

~~Compared to previous work, the analytical solutions presented herein account for an additional degree of freedom in terms of the domain definition: the ice column thickness L. Nonetheless, these solutions should converge under certain conditions to the L-independent solution of Carslaw and Jaeger (1988) if we let $L \to \infty$. For completeness~~We employ identical physical constants to allow for a one-to-one comparison of our results (see Table 1). As thoroughly discussed in Section 7, the vertical gradient of the horizontal velocity determined the applicability of our analytical solution. For this reason, we shall ~~show that~~

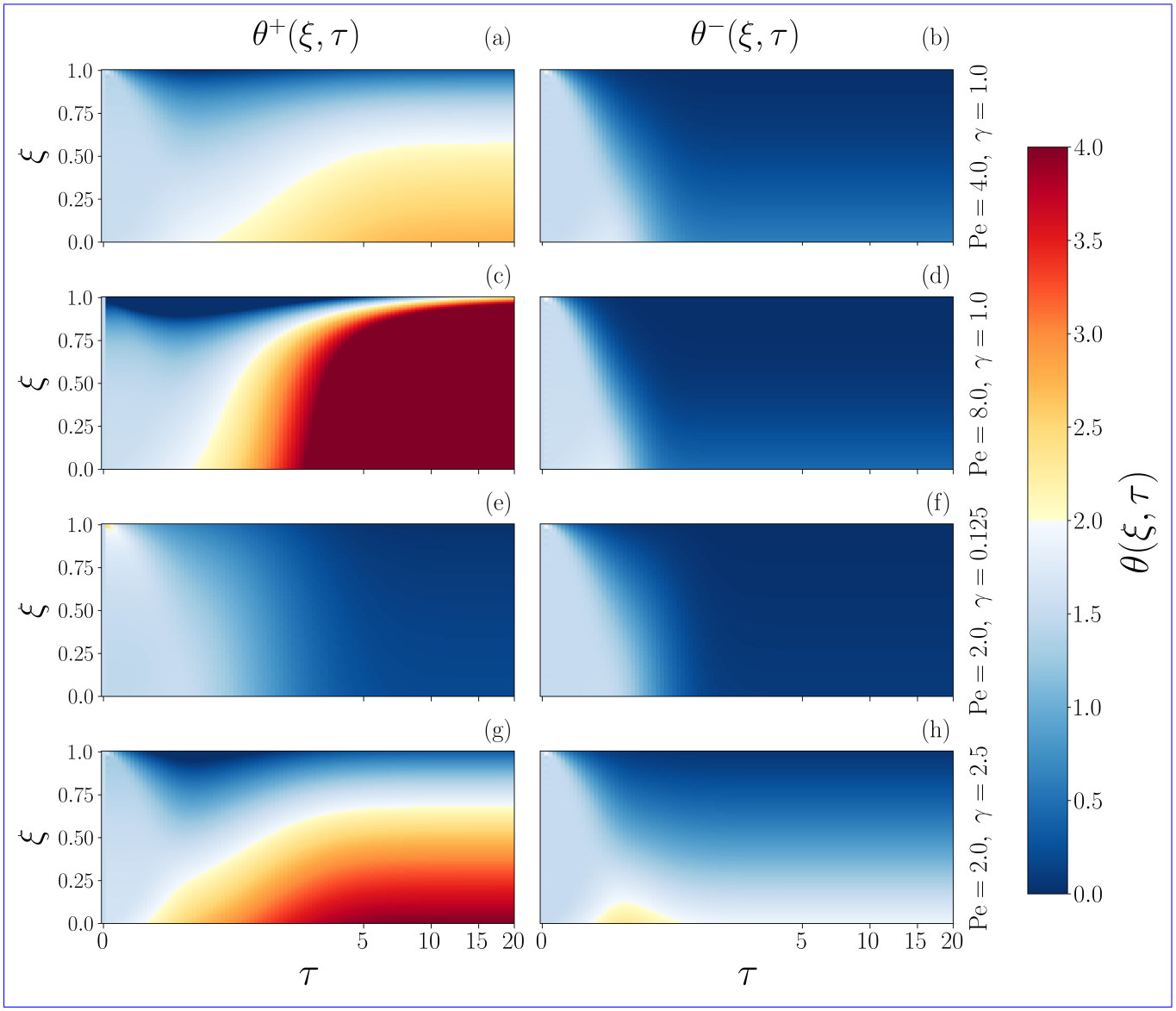

Figure 4. Dimensionless time-dependent solution given an initial temperature profile. For simplicity, here $\theta_0(\xi) = 1.5$ in all cases. Left column: upward advection $w_0 > 0$. Right column: downward advection $w_0 < 0$. Each row represents a particular choice of the non-dimensional numbers Pe and γ.

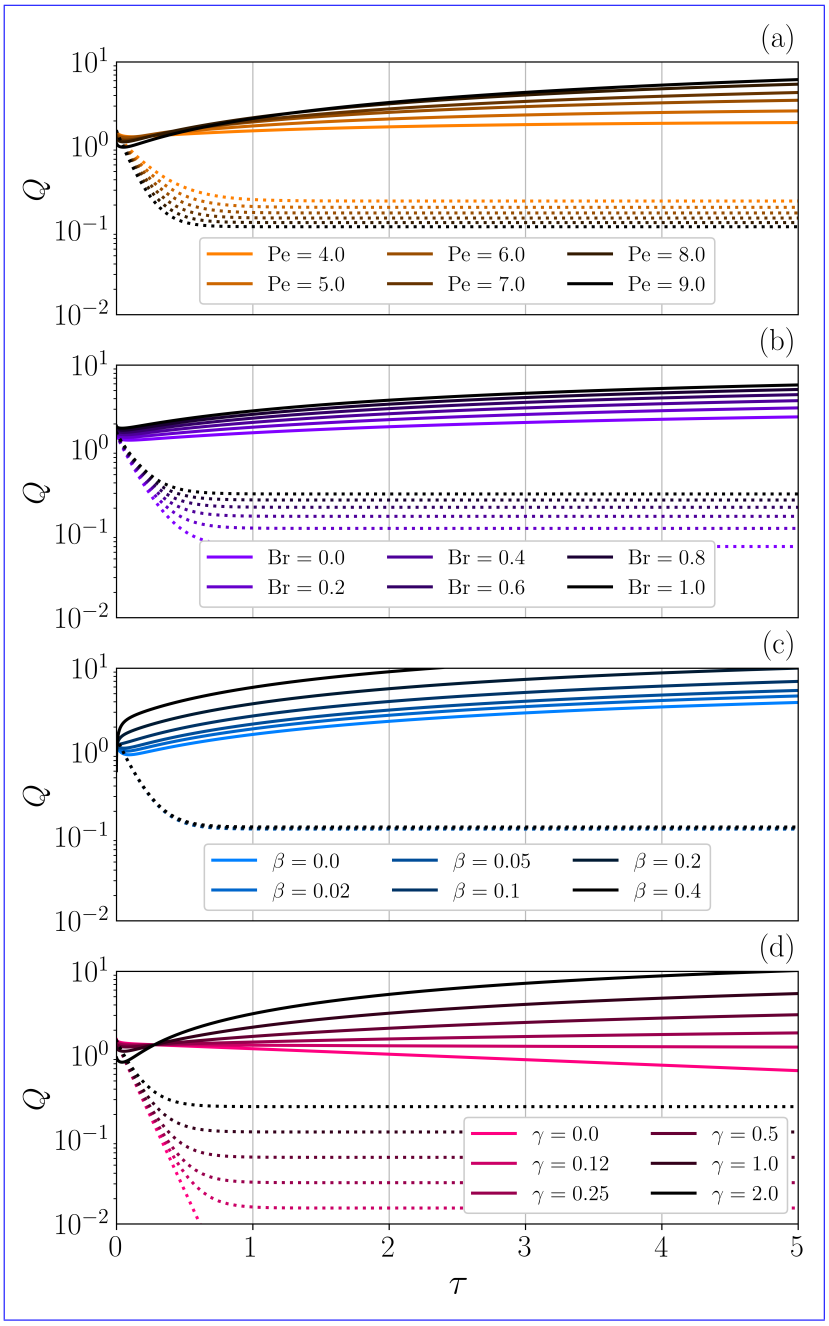

Figure 5. Column energy content as a function of time for the explored range of non-dimensional numbers: (a) Pe, (b) Br, (c) β and (d) γ. Solid line: upward advection ($w_0 > 0$). Dotted line: downward advection ($w_0 < 0$). The energy is obtained through integration of each temperature profile at any given time, so that $Q(\tau) = \int_0^1 \theta(\xi, \tau) d\xi$. Note the y-axis logarithmic scale.

~~Time to reach the pressure melting point as a function of the ice thickness L, initial and boundary conditions in our general formulation. $\beta = 100$ m for all solutions. (Eq. **??**). Boundary conditions: (a) Geothermal heat flux G and (b) Air temperature T_{air}. Initial conditions: (c) Initial ice surface temperature θ_{L} and (d) Initial basal temperature θ_{b}. Each panel represents the dependency of T to the explored range of values given in Table **??** while fixing the remaining variables.~~

~~the theoretical periodicity of MacAyeal (1993a) is in fact retrieved in such limit irrespective of the specific boundary condition at the top.~~ focus on the ice divide results of EISMINT benchmark experiments (Fig. 3 in Huybrechts and Payne, 1996).

~~The particular conditions under which our solution converges must imply an equivalent physical scenario to the one established by MacAyeal (1993a). Specifically, he considered an initial temperature profile that follows an atmospheric lapse rate Γ since the ice column is assumed to be assembled by snow precipitation. Hence the temperature solution is decomposed into a steady and a transient component, corresponding to Γ and the 'excess' of geothermal heat flux $\tilde{G} = G - k\Gamma$ respectively. In addition, pressure melting corrections were not considered. If we account for this particular formulation in our more general approach, the estimated 6944-year-period is retrieved in the limit $L \to \infty$ (Fig. **??**).~~

Table 1. Values of employed physical constants.

Symbol	Value	Quantity
A	10^{16} Pa^{3}yr^{-1}	Pre-exponential flow-law parameter
ρ	910 kg^{3}m^{-3}	Ice density
k	2.1 Wm^{-1}K^{-1}	Thermal conductivity
c_p	2009 J kg^{-1}K^{-1}	Specific heat capacity
T_{air}	239 K	Atmosphere temperature
b	8.7×10^{-4} K m^{-1}	Change of melting point with ice depth
G	42 mK m^{-2}	Geothermal heat flow
w_0	-0.3 m yr^{-1}	EISMINT vertical velocity at the surface
L	~ 3000 m	EISMINT ice thickness

~~Even though the eigenvalues of our problem satisfy a different relation in the limit $\beta = 0$, we shall prove that convergence to the 6944-year-period is independent of β and therefore consistent with previous results. Let φ~~ As noted by the authors, EISMINT modeled temperatures greatly varied particularly near the base. Unfortunately, an independent analytical control on temperature was not available, the reason being a vertical velocity profile (and therefore a strain rate) that did not match the vertical velocity profile obtained if Glen's flow law is employed (Huybrechts and Payne, 1996, Fig. 3 therein). Available analytical solutions are Robin (1955) and Raymond (1983) for a linear and a quadratic vertical velocity profile, respectively. These solutions underestimate and overestimate, respectively. Hence, a vertical velocity field that better matches values modeled with Glen's law must take an exponent between $m = 1$ (linear) and ~~ϕ be two solutions of our general boundary problem (Set 2) with a zero and a non-zero β value respectively and arbitrary initial conditions. The difference between solutions is then:~~

$m = 2$ (quadratic). More generally, we can write:

$$\Delta \doteq \phi - \varphi w(\xi) = \sum_{n=0}^{\infty} A_n \cos\sqrt{\lambda_n} y e^{-\kappa\lambda_n t} - {}_n\cos\sqrt{\tilde{\lambda}_n} y e^{-\kappa\tilde{\lambda}_n t} . w_0 \xi^m \tag{13}$$

where $m > 0$ can be chosen to reproduce the vertical velocity modeled via Glen's flow law (see Fig. 3 in Huybrechts and Payne, 1996)

.

We must recall that the eigenvalues for a non-zero β case In the absence of source term (i.e., ϕ) must satisfy Eq. **??**. With an appropriate change of variable $x_n = L\sqrt{\lambda_n}$, it is clear that:

$$\lim_{L\to\infty}\left[\tan(x_n) = \frac{L}{\beta x_n}\right] \to x_n = \left(n + \frac{1}{2}\right)\pi,$$

since the right hand side goes to zero, we are thus left with roots of $\tan(x_n) = 0$. Note that $n = 0, 1, 2...$, which precisely correspond to the eigenvalues of the $\beta = 0$ case.

Hence, it is straightforward to see that the spatial and temporal dependency in Δ vanish in the limit $L \to \infty$. Additionally, given that the only L-order term is not proportional to β in the initial conditions, $\Omega = 0$) as in the EISMINT experiments, we can provide analytical solutions of the coefficients A_n temperature distribution for a general power-law dependency of the vertical velocity (derivation details in Appendix C):

$$\vartheta^-(\xi) = \frac{p\gamma}{(pw_0)^p}\,\Gamma\left(p, pw_0\xi^{m+1}\right) + C \tag{14}$$

where $\Gamma(n, x)$ is the incomplete Gamma function (e.g., Abramowitz and Stegun, 1965), $p = (m+1)^{-1}$ and $\tilde{A}_n$ become identical in such a limit. We then conclude that $\Delta = 0$ if β is finite as $L \to \infty$. In other words, we have proven that both solutions are asymptotically equivalent irrespective of β as the ice thickness approaches infinity. C is a constant given by the top boundary condition (see Appendix C).

MacAyeal (1993a) seemingly showed that the boundary conditions and This general solution allows us to study the exponent m that best matches the EISMINT modeled vertical velocity. Figure 6 shows a number of vertical velocities and their corresponding temperature profile at equilibrium. We retrieve Robin (1955) and Raymond (1983) for $m = 1$ and $m = 2$, respectively. We must stress that a vertical velocity profile with an exponent $m = 1.5$ closely matches the velocity field modeled with Glen's flow law and yields a temperature profile nearly identical to the temperature distribution calculated in EISMINT. Temperature profiles substantially differ from Robin (1955) and Raymond (1983) solutions, thus showing the critical choice of power-law exponent m, particularly near the base. In fact, we find that the upper 40% of the ice base temperature are decoupled by estimating that the e-fold decay of a periodic forcing with $\omega = 2.84 \times 10^{-11}\ s^{-1}$ in a motionless column reads $\sqrt{2k/\omega} = 314$ m. This estimation solely considers periodic signals, whilst leaving unexplored the implication of a non-periodic forcing.Our results affirm otherwise: though an oscillatory forcing rapidly attenuates with depth, Fig. **??** and **??** show that the base is in fact strongly coupled with both the external conditions and the initial thermal state of the ice. The strength of this coupling is determined by the column thickness L and the subsequent boundary conditions.

Figure **??** further shows that the ice thickness at which decoupling between the surface and the base occurs is almost independent of the top boundary conditions. In other words, we find that for MacAyeal (1993a)'s choice of geothermal heat flux $\tilde{G}$ (Table **??**), the base evolves irrespective of the surface conditions for values $L > 3.0$ kmcolumn is irrespective of the particular z-dependency of the vertical velocity.

~~Time required for the column base to thaw as a function of the ice column thickness L. This timescale is classically considered to be the period of a binge-purge oscillator, a potential mechanism behind the Heinrich Events. Colours represent the air temperature: $T_{\mathrm{air},1} = -40$ºC, $T_{\mathrm{air},2} = -30$ºC and $T_{\mathrm{air},3} = -20$ºC. Solid line represents solutions for $\beta = 100$ m whereas the case $\beta = 0$ (i.e., fixed surface temperature) is denoted by a dotted line. The boundary condition at the base $\theta_y = -G/k$ is identical for all cases.~~

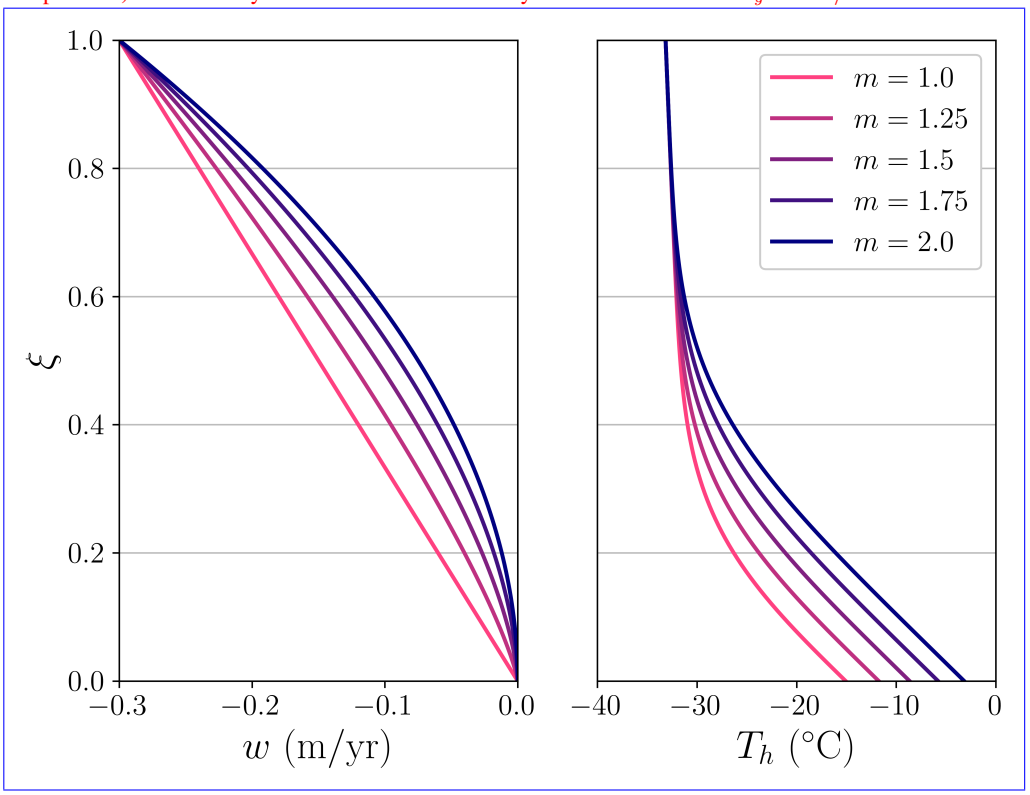

Figure 6. Left panel: vertical velocity profiles of the form $w(\xi) = w_0 \xi^m$ for five different values of the exponent $m = 1.0, 1.25, 1.50, 1.75, 2.0$. Velocity magnitude at the surface reads $w_0 = -0.3$ m/yr (i.e., downwards advection). Robin (1955) vertical velocity assumption corresponds to $m = 1$, whereas Raymond (1983) employs $m = 2$. Right panel: homologous ice temperature T_h at equilibrium as given by solution in Eq. 14 after dimensionalisation of $\vartheta^-(\xi)$.

7 ~~Conclusions~~

7 Discussion

The adoption of dimensionless variables results in enhanced generality and mathematical convenience, albeit at the expense of veiling the practical significance to real glaciers and ice sheets. We have consequently tabulated data for characteristic values to ease interpretation (Table 2), thus showing that the explored range encompasses realistic values found in ice caps.

~~We have considered the implications of a finite one-dimensional ice column domain with a given thickness L on the solutions of Fourier heat equation. The main purpose of the current work is to advance our understanding of how the thickness of an ice sheet influences its thermal evolution and further reconsider an important foundational piece of literature in the binge-purge hypothesis (MacAyeal, 1993a, b) in the more realistic setup of a finite thickness ice column and more general (Robin)boundary conditions. Unlike previous work, we provide analytical solutions that are explicitly dependent on this new degree of freedom L, thus quantifying its relevance without further approximations~~We first start by comparing our results with a previously obtained solution for a simpler case (e.g., Clarke et al., 1977). We obtain identical results by setting the ice surface temperature to a fixed value given by the air temperature, i.e., setting $\beta = 0$ in Eq. 2 (Figs. 2c and 2f). Prominently, not only the ice surface but also the entire column is perturbed for a non-zero β value. This further implies that the thermal state of the base is sensitive to the particular energy balance at the ice-air interface for the upward advective scenario. On the contrary, under downwards advective conditions, the thermal basal equilibrium is found irrespective of the specific top boundary condition (Figs. 2e, 2f and 2g), provided a null strain heating rate. If the latter condition is relaxed, then the base becomes warmer as the insulating parameter β increases (Fig. 2h).

~~As a result of our new domain definition, we have studied physically-plausible scenarios imposed by a more general (Robin) boundary condition at the top of the motionless ice column. This approach considers that the ice and the air may not be always at thermal equilibrium, thus yielding a heat flux across the interface due to a vertical temperature gradient . As a result, both the ice temperature at the top and its vertical gradient are allowed to vary in time. If the ice surface happens to reach the air temperature ,~~ Even though the equilibration time depends on the particular initial state, the downward advective case seems to converge to the stationary solution faster than the upward scenario irrespective of the particular insulating value at the ice surface (Fig. 5). This entails that under downward advective conditions, the overall balance of energy exchange is solely dictated by the air temperature, the geothermal heat flux and the ice vertical velocity, thus dismissing any potential surface insulating effects.

The tractability of the analytical solution does not allow for further complexity and hence additional numerical methods would be necessary if such a physical description is desired. Nonetheless, a constant horizontal advection term was also introduced as part of the inhomogeneous term Ω, for which the sign of the horizontal temperature gradients must be chosen a priori. Even though horizontal variability of temperature distributions can vary greatly, we account for this effect assuming a constant term (throughout the ice column) entering the heat equation, thus not reflecting much of the non-local features of the thermal structure of the ice sheets.

We must stress that the our analytical solutions are not limited to regions with negligible horizontal velocities, since the true constraining quantity is the vertical ~~gradient vanishes leading to a thermal equilibrium state.~~ gradient of the horizontal velocity u_z. Hence, rapid sliding regions with a nearly constant horizontal velocity throughout the vertical axis are also suitably described by our solutions, for that $u_z \simeq 0$ implies that the temperature profile is merely transported along the flow direction, while keeping the shape of the vertical temperature distribution. One can argue that the additional source of heat due to frictional dissipation should be now also considered. Nonetheless, in terms of temperature distribution, this effect is equivalent to an increased geothermal heat flux as it is purely restricted to the column base and therefore already encompassed in Eq. A.1.

~~We find that the ice thickness plays a fundamental role in the Fourier solutions, which implies that a semi-infinite domain is an oversimplification (for the ice thickness range present in nature). The temperature at the base is highly dependent on the particular boundary condition at the top of the ice column. Particularly~~It is worth noting that phase changes are not herein considered, so that temperature evolution is strictly confined to values below the pressure-melting point. Unlike a numerical solver, where temperature is manually limited, these solutions ~~are significantly distinct from each other for ice thicknesses $L < 2$ km.~~ must be taken with cautious as we are describing a frozen ice column. Results are still compatible with a potential heat contribution due to basal frictional heat Eq. 2, for that fast sliding regions are often related with temperate basal conditions. Nevertheless, an additional contribution would imply an increased vertical temperature gradient even if the column base eventually reached the pressure-melting point.

~~Our analytical approach allows us to quantify the sensitivity of the solution both to the initial and boundary conditions. In our particular parameter choice, the thermal state of the base completely decouples from the upper boundary condition (i.e., external forcing) for L values above 2 km and its thermal evolution becomes solely a function of the lower~~ The potential existence of an insulating firn layer at the surface presents a physical justification for the new top boundary condition (~~i. e.~~ Eq. 1). Ice forms by snow densification through time (see review in Stevens et al., 2020), ~~the geothermal heat flux). A distinct choice will alter this value, yet we expect this behaviour to remain present.~~

~~Notably, in the limit $L \to \infty$, the prior L-independent solution (Carslaw and Jaeger, 1988) is retrieved, consequently yielding the 6944 years periodicity estimated by MacAyeal (1993a). For completeness, we showed that such periodicity is in fact retrieved irrespective of the particular boundary condition at the top. This confirms the robustness of our results.~~

~~Regarding a potential estimation of the binge-purge periodicity based on our analytical solutions, the new degree of freedom L entails strong consequences. First, large temporal variability can be explained solely by considering a change in ice thickness without any additional factors. In other words, this provides a source of natural internal variability irrespective of the external forcing. For a 1-4 km thick ice sheets, this variability spans a 7-12 kyr range. In addition,~~ thus yielding layers of progressively increasing density descending from the surface. Likewise, snow thermal conductivity increases with density (e.g., Sturm et al., 1997), resulting in a poor heat conductor as the snow-air interface is approached. As already noted by Carslaw and Jaeger (1988), if the flux across a surface is proportional to the temperature difference between the surface and the surrounding medium, the ~~explicit consideration of distinct initial temperature profiles manifests a high sensitivity of the binge-purge oscillator period to its initial state.~~ appropriate boundary condition takes the form of Eq. 1, rather than the oversimplified version $\theta(L,t) = T_{\mathrm{air}}$.

Here we explicitly describe the ice column with a constant thermal conductivity, but we allow for a firn layer to be treated as a thin surface skin of poor conductivity (equivalent to Chapter I, Carslaw and Jaeger, 1988). Nonethless, when $\beta = 0$ is imposed, the traditional approach with no firn layer is recovered.

~~Moreover, a finite thickness also determines the mechanism by which an atmospheric perturbation might potentially influence the time required to melt the ice base since we have quantified the effect of a prescribed surface temperature and a vertical gradient. For a fixed L value, besides the geothermal heat flux, both the vertical gradient and the temperature at the top govern the~~ Our practical exercise with the EISMINT benchmark illustrates the importance of the analytical solutions. Previously obtained solutions have strong assumptions on how vertical velocity changes with column height: linear (Robin, 1955) and quadratic (Raymond, 1983) vertical velocity profiles (exponents $m = 1$ and $m = 2$ in Fig. 6). Therefore, they respectively overestimate and underestimate the velocity field modeled with Glen's flow law. In order to obtain a more accurate vertical velocity, we solve for the temperature ~~time evolution, consequently defining the particular binge-purge periodicity estimation.~~ allowing for intermediate values of the exponent to capture a behaviour that lies amidst a linear and a quadratic dependency. Our results show that for the choice $m = 3/2$, we obtain a nearly identical velocity field and consequently a temperature profile that fairly reproduces the mean profile in EISMINT benchmark. Solutions herein presented are thus applicable to a wide range of vertical velocity distributions and can be chosen simply by modifying the exponent value m.

~~It must be stressed that even though we have shown that the ice base temperature is in fact coupled with the boundary conditions,~~

Table 2. Non-dimensional definitions, characteristic range and EISMINT corresponding values (see also Table 1). Summation is implied over repeated indices.

Symbol	Definition	Characteristic range	EISMINT
Pe	$\frac{L}{\kappa} w_0$	$0.0 - 30.0$	26.07
Br	$\frac{L^2}{\kappa T_{\text{air}}} \sigma_{ij} \dot{\epsilon}_{ij}$	$0.0 - 1.0$	0.0
Λ	$\frac{L^2}{\kappa T_{\text{air}}} \int_0^1 (\mathbf{u} \cdot \hat{\mathbf{n}}) \theta_{\hat{\mathbf{n}}} \, d\xi$	$0.0 - 0.01$	0.0
γ	$-\frac{T_{\text{air}}}{kL} \Upsilon$	$0.125 - 2.0$	1.90
β	$\frac{\beta}{L}$	$0.0 - 0.125$	0.0

8 Conclusions

We have determined the analytical solution to the 1D time-dependent advective-diffusive heat problem including a source term due to strain rate deformation and a more realistic set of boundary conditions. The solution was expressed in terms of confluent hypergeometric functions following a separation of variables approach. Non-dimensionalisation reduced the parameter space to four numbers that fully determine the shape of the solution at equilibrium. The transient component additionally depends on the initial temperature distribution and exponentially converges to the stationary solution.

The sign of the vertical advection is of utmost importance as it determines the direction along which temperature gradients are transported. Notably, the ~~periodicity of the HE cannot be imposed by the frequency of an external forcing~~ particular boundary condition at the ice surface is irrelevant in a downward advective scenario, unless an additional source of heat within the column is present (i.e., $\mathrm{Br} \neq 0$). This implies that regions with negligible strain heating rates present a similar temperature distribution for the uppermost part of the column regardless of the particular geothermal heat flux value. This is true even for highly insulating conditions at the ice surface~~. Rather, the timescale to reach melting conditions is determined by the ice thickness and the energy condition at the base and the surface~~, where colder ice is transported more efficiently than heat travels upwards due to diffusion.

The transient regime also differs regarding the sign of the advective term. Our energy content study reveals that downward advection is a much more efficient manner of changing the energy content as the thermal equilibrium is reached earlier compared to the upwards scenario. This holds true for all parameter values herein explored.

~~Lastly, we note that a subtle connection exists between internal free (the binge-purge hypothesis) and externally-driven (in the sense of a time-dependent boundary condition at the top) mechanisms caused by the finitude of the domain. Since thermomechanical instabilities (i.e. ,~~ Unlike prior studies, our analytical approach allows us to quantify the relative importance of each non-dimensional parameter both at equilibrium and during the transitory regime. Peclét number (both sign and magnitude) and γ dictate the temperature distribution of the ~~transition between two plausible stages of basal lubrication governed by the thermal state of the ice) are the triggering mechanism of a binge-purge oscillator, internal free oscillations are sensitive to the particular climatic forcing imposed as a boundary condition at the top of the ice column. This double-fold nature of thermomechanical instabilities is only exhibited when a finite domain is considered, further supporting the use of such analytical solutions in simple low-dimensional ice-sheet models where temperature profiles are otherwise prescribed~~ice column during the first instants of the transitory regime. As this time-dependent solution vanishes, the slower effect of strain heating rate and the surface insulating parameter become relevant to determine the stationary shape of the temperature profile.

A practical example based on EISMINT benchmark experiments eases the interpretation of our dimensionless formulation and illustrates the relevance of the analytical solutions presented herein. By employing the incomplete Gamma function, we are able to provide exact solutions for a general power-law formulation of the vertical velocity profile. This takes a step forward on the analytical temperature control available in the literature, previously limited to a linear and a quadratic dependency. We find that the vertical velocity profile with an exponent $m = 3/2$ closely matches the velocity field modeled with Glen's flow law

and yields a temperature profile nearly identical to the temperature distribution calculated in EISMINT. This result thus yields an independent analytical control of the temperature, applicable to real vertical velocity profiles obtained via Glen's flow law.

Lastly, we note that our analytical solutions are general and can be applied to any initial boundary value problem that fulfils the conditions herein described. They can provide temperature distributions for any 1D problem at arbitrarily high spatial and temporal resolutions, that considers the combined effects of diffusion, advection and strain heating without any additional numerical implementation. Furthermore, they present a reliable benchmark test for any numerical thermomecanical solver to quantify accuracy losses and necessary spatial and temporal resolutions.

Code availability. TEXT

Data availability. TEXT

Code and data availability. All scripts to obtain the results herein presented and to further plot figures can be found in: https://github.com/d-morenop/Suplementary_ice-column-thermodynamics

Sample availability. TEXT

Video supplement. TEXT

Appendix A: Separation of variables and full solution

Let us briefly outline the separation of variables technique before elaborating on the solutions of our general problem. Consider the following initial/boundary problem on an interval $\mathcal{I} \subset \mathbb{R}$,

$$\begin{cases} \mu_\tau = \mu_{\xi\xi} - w\mu_\xi, & \xi \in \tilde{\mathcal{L}},\ \tau > 0, \\ \mu = \mu_0, & \xi \in \tilde{\mathcal{L}},\ \tau = 0, \\ \mu_\xi = 0, & \xi = 0,\ \tau > 0, \\ \beta\mu_\xi + \mu = 0, & \xi = 1,\ \tau > 0, \end{cases} \tag{A.1}$$

This technique looks for a solution of the form:

$$u\mu(y\xi, t\tau) = Y X(y\xi)T(t\tau), \tag{A.2}$$

where the functions Y and T are to be determined. Assuming that there exists a solution of A.8 and plugging the function ~~$u = YT$~~ $\mu = XT$ into the heat equation, it follows:

$$\frac{T'}{\kappa T}\frac{T_\tau}{T} = \frac{Y''}{Y}\frac{X_{\xi\xi}}{X} - w\frac{X_\xi}{X} = -\lambda, \tag{A.3}$$

for some constant λ. Thus, the solution ~~$u(y,t) = Y(y)T(t)$~~ $\mu(\xi,\tau) = X(\xi)T(\tau)$ of the heat equation must satisfy these equations. ~~Additionally, in order for u to satisfy the boundary conditions, we arrive to:~~

$$\begin{cases} Y''(y) = -\lambda Y(y) & y \in \mathcal{I} \\ Y \text{ satisfies our BCs.} \end{cases}$$

~~This is a well-known eigenvalue problem. Namely, a constant λ that satisfies Eq. **??** for some function X (not identically zero) is called an eigenvalue of $-\partial_y^2$ for the given boundary conditions. Hence, the function Y is an eigenfunction with associated eigenvalue λ.~~

~~Therefore, in~~ In order for a function of the form ~~$u(y,t) = Y(y)T(t)$~~ $\mu(\xi,\tau) = X(\xi)T(\tau)$ to be a solution of the heat equation on the interval $\mathcal{I} \subset \mathbb{R}$, ~~$T$~~ $T(\tau)$ must be a solution of the ODE ~~$T' = -\kappa\lambda T$~~ $T_\tau = -\kappa\lambda T$. Direct integration leads to:

$$T(t\tau) = Ae^{-\kappa\lambda t - \kappa\lambda\tau}, \tag{A.4}$$

for an arbitrary constant A.

Additionally, in order for $\mu(\xi,\tau)$ to satisfy the boundary conditions, we arrive to a second-order linear ordinary differential equation:

$$\begin{cases} X_{\xi\xi}(\xi) - w(\xi)X_\xi(\xi) + \lambda X(\xi) = 0, & \xi \in \tilde{\mathcal{L}}, \\ X_\xi = 0, & \xi = 0, \\ \beta X_\xi + X = 0, & \xi = 1, \end{cases} \tag{A.5}$$

It is necessary to provide the particular shape of the the function $w(\xi)$. First, we will employ the linear profile $w(\xi) = w_0\xi$ so that the differential equation now reads $X_{\xi\xi}(\xi) - w_0\xi X_\xi(\xi) + \lambda X(\xi) = 0$. This equation can be easily identified with the well-known confluent hypergeometric differential equation (e.g., Abramowitz and Stegun, 1965; Evans, 2010) defined as:

$$\xi X_{\xi\xi} + (\delta - \xi)X_\xi - \alpha X = 0, \tag{A.6}$$

Simply by defining $\alpha = -\lambda/(2w_0)$, $\delta = 1/2$ and $\zeta = w_0\xi^2/2$, we can write our solution in terms of the two independent Kummer and Tricomi functions:

$$X(\xi) = C_1\Phi(\alpha,\delta,\zeta) + C_2\Psi(\alpha,\delta,\zeta) \tag{A.7}$$

where C_1 and C_2 are constants to be determined from the boundary conditions. At the base, the solution must vanish, so we set $C_2 = 0$ given that Tricomi function $\Psi(\alpha,\delta,\zeta)$ diverges at the origin. The second boundary condition (i.e., at $\xi = 1$) allows us to determine the eigenvalues λ_n of the problem as we look for all values of α_n that satisfy:

$$\beta\Phi_\xi(\alpha_n,\delta,\zeta) + \Phi(\alpha_n,\delta,\zeta) = 0, \text{ at } \xi = 1, \tag{A.8}$$

and then we compute the eigenvalues $\lambda_n = -2w_0\alpha_n$. This is in fact a trascendental equation with no algebraic representation and therefore, the values of α_n are numerically determined.

Thus, for each eigenfunction ~~Y_n~~ X_n with corresponding eigenvalue λ_n, we have a solution T_n such that:

$$u\mu_n(y\xi, t\tau) = Y X_n(y\xi)T_n(t\tau), \tag{A.9}$$

is a solution of the heat equation on our interval $\mathcal{I}$ which satisfies the BC. Moreover, given that the problem A.8 is linear, any finite linear combination of a sequence of solutions ~~$\{u_n\}$~~ $\{\mu_n\}$ is also a solution. In fact, it can be shown that an infinite series of the form:

$$u\mu(y\xi, t\tau) \equiv \sum_{n=1}^{\infty} u_{n=0}\mu_n(y\xi, t\tau), \tag{A.10}$$

will also be a solution of the heat equation on the interval $\mathcal{I}$ that satisfies our BC, under proper convergence assumptions of this series. The discussion of this issue is beyond the scope of this work.

Appendix B: ~~Solution of the problem~~

~~Let us elaborate on the solution of our general problem (Section ??) by first solving the associated eigenvalue problem. As we employ the separation of variables technique, the solution takes the form :~~

$$\xi(y,t) = \sum_{n=0}^{\infty} Y_n(y)T_n(t),$$

We can then express the transitory solution as:

$$\theta(\xi,\tau) = \sum_{n=0}^{\infty} A_n\Phi(\alpha_n;\delta;\zeta)\, e^{-\lambda_n\tau} \tag{A.1}$$

where the functions $Y_n(y)$ and $T_n(t)$ are to be determined. After the consequent change of variable so that $Y(y)$ satisfies Eq. ??, we arrive to : where the coefficients A_n are given by the initial condition.

Since the confluent hypergeometric functions are orthogonal, the normalized eigenfunctions form an orthonormal basis under the $\varrho(\xi)$-weighted inner product in the Hilbert space L^2, thus allowing to write the coefficients A_n as:

$$Y A_n = \frac{1}{||\Phi_n||^2} \int_0^1 \left(\theta(y\xi, 0) - \vartheta(\xi) = A_n \cos\sqrt{\lambda_n} y \right) + B_n \sin\varrho(\xi) \Phi\left(\sqrt{\lambda_n} y \alpha_n; \delta; \zeta \right), d\xi. \tag{A.2}$$

where A_n and B_n are to be determined. Applying the boundary conditions imposed in Set 2, it is clear that all sine coefficients are identically zero $B_n = 0$ and the eigenvalues $\sqrt{\lambda_n}$ are given by the transcendental equation:

Appendix B: Stationary solution

For the stationary regime, we do not need to apply separation of variables for that the problem reduces to a second-order ordinary differential equation in only one independent variable ξ:

$$\begin{cases} \Omega = \vartheta_{\xi\xi} - w\vartheta_\xi, & \xi \in \tilde{\mathcal{L}}, \\ \vartheta_\xi = \gamma, & \xi = 0, \\ \beta\vartheta_\xi + \vartheta = 1, & \xi = 1, \end{cases} \tag{B.1}$$

Even though the eigenvalues we have increased the complexity of the problem are given by a trascendental equation with no algebraic representation, $\xi(y, 0)$ is a function of the form $f(y) = a + by$ and the coefficients A_n yield an explicit integration:

$$A_n = \frac{2}{L} \frac{\sqrt{\lambda_n}(a + bL)\sin\left(\sqrt{\lambda_n} L\right) + b\cos\left(\sqrt{\lambda_n} L\right) - b}{\lambda_n}$$

where $a = G/k + (\theta_{\mathrm{L}} - \theta_{\mathrm{sl}})$ and $b = \theta_{\mathrm{sl}} - T_{\mathrm{air}} - (\beta + L)G/k$.

Hencewith a refined top boundary condition and non-homogeneous term Ω, the solution of our general problem reads:

can still be found analytically:

$$\xi\vartheta(y, t\xi) = \sum_{n=0}^{\infty} A_n \cos\Omega \frac{\xi^2}{2} {}_2F_2\left(\sqrt{\lambda_n} y e^{-\kappa\lambda_n t} 1, 1; \frac{3}{2}, 2; -\zeta \right) + A \operatorname{erf}\left[a\xi \right] + B \tag{B.2}$$

where ${}_2F_2(a_1, a_2; b_1, b_2, x)$ is the generalised hypergeometric function, $\zeta = (a\xi)^2$, $a = (w_0/2)^{1/2}$, $A = -\gamma(\pi/(4a))^{1/2}$ and $B = 1 - A\left(2a\pi^{-1}\beta e^{-a^2} + \operatorname{erf}[a]\right) - \Omega\left((\beta + 1/2)\,{}_2F_2(1, 1; 3/2, 2, a^2) + \beta a^2\,{}_2F_2(2, 2; 5/2, 3, a^2)/3\right)$ is a constant given by the top boundary condition. Note that hypergeometric function can be easily differentiated following e.g., Eq. 15.2.1 in Abramowitz and Stegun (1965).

Appendix C: ~~Limit case $\beta = 0$~~

~~It is crucial to consider that the eigenvalue equation given by Eq. ?? does not hold for $\beta = 0$. In such case, after the consequent change of variable so that $Y(y)$ satisfies Eq.??, we arrive to:~~

$$Y_n(y) = A_n \cos\left(\sqrt{\lambda_n} y\right) + B_n \sin\left(\sqrt{\lambda_n} y\right),$$

~~where A_n and B_n are to be determined. Applying the boundary conditions imposed in Set 2, it is clear that all sine coefficients are identically zero, $B_n = 0$, and the eigenvalues read:~~

Appendix C: EISMINT stationary solution

In this section, we also assume thermal equilibrium, thus reducing again the problem to a second-order ordinary differential equation in only one independent variable ξ:

$$\sqrt{\lambda_n} = n + \frac{1}{2}\frac{\pi}{L}, \begin{cases} 0 = \vartheta_{\xi\xi} - w\vartheta_{\xi}, & \xi \in \tilde{\mathcal{L}}, \\ \vartheta_{\xi} = \gamma, & \xi = 0, \\ \beta\vartheta_{\xi} + \vartheta = 1, & \xi = 1, \end{cases} \tag{C.1}$$

where ~~$n = 0, 1, 2, ...$~~we have set $\Omega = 0$ for a one-to-one comparison with EISMINT benchmark experiments.

~~From orthogonality of the eigenfunctions $Y_n(y)$, the coefficients A_n of our solution are calculated following:~~

Unlike the general stationary solution shown in Eq. B.2, we allow for a general power-law vertical velocity profile of the form $w(\xi) = w_0 \xi^m$. The solution can be then expressed as:

$$A_n = \frac{2}{L}\int_0^L \xi\vartheta^-(y,0\xi) = \frac{p\gamma}{(pw_0)^p}\cos\Gamma\left(\sqrt{\lambda_n} yp, pw_0\xi^{m+1}\right) dy. + C \tag{C.2}$$

where ~~$\xi(y,0) = \frac{\tilde{G}}{k}(y - L) - \theta_L + \theta_b$. Since $\xi(y,0)$ is a function of the form $f(y) = ay + b$ and the eigenvalues allow for an analytical expression, the integration of the coefficients A_n is straightforward:~~

$p = (m+1)^{-1}$, $C = 1 - [2\beta(pw_0)^p e^{-pw_0} + \Gamma(p, w_0 p)]p\gamma/(pw_0)^p$ is a constant given by the top boundary condition and $\Gamma(\cdot,\cdot)$ is the upper incomplete gamma function defined as:

$$A_n\Gamma\left(a, x\right) = \frac{4(\theta_b - \theta_L)}{2n\pi + \pi}\cos(n\pi) - 8L\frac{\tilde{G}}{k}\frac{1}{2n\pi + \pi}^2 \cdot \int_x^\infty e^{-t}t^{a-1}dt \tag{C.3}$$

~~It is clear that this series converges and satisfies the initial condition imposed by $\xi(y,0)$ given that:~~

$$\sum_{n=0}^{\infty} \frac{\cos(n\pi)}{2n\pi+\pi} = \frac{1}{4},$$

$$\sum_{n=0}^{\infty} \frac{1}{(2n\pi+\pi)^2} = \frac{1}{8}.$$

Additionally, the solution can be also expressed in terms of Kummer confluent hypergeometric function Φ given the relation (Abramowitz and Stegun, 1965, Eqs. 6.5.3 and 6.5.12):

$$\Gamma(a,x) = \Gamma(a) - a^{-1}x^a e^{-x}\Phi(1,1+a;x) \tag{C.4}$$

Hence, the ~~solution of Problem 1 reads:~~

$$\zeta(y,t) = \sum_{n=0}^{\infty} A_n \cos\left(\sqrt{\lambda_n} y\right) e^{-\kappa\lambda_n t},$$

stationary solution is equivalent to $\sim \Phi\left(1, p+1; p w_0 \xi^{m+1}\right)$.

Author contributions. Daniel Moreno-Parada formulated the problem, derived the analytical solutions, analysed the results and wrote the paper. All other authors contributed to analyse the results and writing the paper.

Competing interests. Alexander Robinson is an editor of The Cryosphere. The peer-review process was guided by an independent editor, and the authors have also no other competing interests to declare.

Disclaimer. TEXT

Acknowledgements. This research has been supported by the Spanish Ministry of Science and Innovation (project IceAge, grant no. PID2019-110714RA-100), the Ramón y Cajal Programme of the Spanish Ministry for Science, Innovation and Universities (grant no. RYC-2016-20587) and the European Commission, H2020 Research Infrastructures (TiPES, grant no. 820970).

References

Abramowitz, M. and Stegun, I.: Handbook of Mathematical Functions: With Formulas, Graphs, and Mathematical Tables, Applied mathematics series, Dover Publications, https://books.google.es/books?id=MtU8uP7XMvoC, 1965.

Al-Niami, A. and Rushton, K.: Analysis of flow against dispersion in porous media, Journal of Hydrology, 33, 87–97, https://doi.org/10.1016/0022-1694(77)90100-7, 1977.

Alley, R. and Whillans, I.: Changes in the West Antarctic ice sheet, Science, 254, 959, 1991.

Aral, M. M. and Liao, B.: Analytical Solutions for Two-Dimensional Transport Equation with Time-Dependent Dispersion Coefficients, Journal of Hydrologic Engineering, 1, 20–32, 1996.

Banks, R. B. and Ali, I.: Dispersion and adsorption in porous media flow, J. Hydraul. Div., Am. Soc. Civ. Eng.; (United States), 90:HY5, https://www.osti.gov/biblio/6949390, 1964.

Bear, J.: Dynamics of Fluids in Porous Media, Soil Science, 120, 162–163, 1975.

Bougamont, M., Price, S., Christoffersen, P., and Payne, A. J.: Dynamic patterns of ice stream flow in a 3-D higher-order ice sheet model with plastic bed and simplified hydrology, Journal of Geophysical Research, 116, https://doi.org/10.1029/2011jf002025, 2011.

Brent, R.: Brent, Richard P. An algorithm with guaranteed convergence for finding a zero of a function., The computer journal, 14, 422–425, 1971.

Calov, R., Greve, R., Abe-Ouchi, A., Bueler, E., Huybrechts, P., Johnson, J. V., Pattyn, F., Pollard, D., Ritz, C., Saito, F., and Tarasov, L.: Results from the Ice-Sheet Model Intercomparison Project–Heinrich Event Intercomparison (ISMIP HEINO), Journal of Glaciology, 56, 371–383, https://doi.org/10.3189/002214310792447789, 2010.

Carslaw, H. S. and Jaeger, J. C.: Conduction of heat in solids, Clarendon Press, Oxford, 1988.

Clarke, G. K. C., Nitsan, U., and Paterson, W. S. B.: Strain heating and creep instability in glaciers and ice sheets, Reviews of Geophysics, 15, 235, https://doi.org/10.1029/rg015i002p00235, 1977.

Debnath, L. and Bhatta, D.: Integral Transforms and Their Applications, Third Edition, Taylor & Francis, https://books.google.es/books?id=tGpYBQAAQBAJ, 2014.

Dekker, T.: Finding a zero by means of successive linear interpolation., Constructive Aspects of the Fundamental Theorem of Algebra, B. Dejon and P. Henrici, Eds., Wiley Interscience, London, 1969.

Evans, L.: Partial Differential Equations, Graduate studies in mathematics, American Mathematical Society, https://books.google.es/books?id=Xnu0o_EJrCQC, 2010.

Glovinetto, M. B. and Zwally, H. J.: Spatial distribution of net surface accumulation on the Antarctic ice sheet, Annals of Glaciology, 31, 171–178, https://doi.org/10.3189/172756400781820200, 2000.

Greve, R. and Blatter, H.: Dynamics of Ice Sheets and Glaciers, Springer Berlin Heidelberg, https://doi.org/10.1007/978-3-642-03415-2, 2009.

Gustafson, K. and Abe, T.: The third boundary condition—was it robin's?, The Mathematical Intelligencer, 20, 63–71, https://doi.org/10.1007/bf03024402, 1998.

Guvanasen, V. and Volker, R. E.: Experimental investigations of unconfined aquifer pollution from recharge basins, Water Resources Research, 19, 707–717, https://doi.org/10.1029/wr019i003p00707, 1983.

Harleman, D. R. F. and Rumer, R. R.: Longitudinal and lateral dispersion in an isotropic porous medium, Journal of Fluid Mechanics, 16, 385–394, https://doi.org/10.1017/S0022112063000847, 1963.

Hughes, T.: On the pulling power of ice streams, Journal of Glaciology, 38, 125–151, https://doi.org/10.3189/s0022143000009667, 1992.

Huybrechts, P. and Payne, T.: The EISMINT benchmarks for testing ice-sheet models, Annals of Glaciology, 23, 1–12, https://doi.org/10.3189/S0260305500013197, 1996.

Joughin, I., Tulaczyk, S., Bindschadler, R., and Price, S. F.: Changes in west Antarctic ice stream velocities: Observation and analysis, Journal of Geophysical Research: Solid Earth, 107, EPM 3–1–EPM 3–22, https://doi.org/10.1029/2001jb001029, 2002.

Joughin, I., MacAyeal, D. R., and Tulaczyk, S.: Basal shear stress of the Ross ice streams from control method inversions, Journal of Geophysical Research: Solid Earth, 109, n/a–n/a, https://doi.org/10.1029/2003jb002960, 2004.

Kalnins, E. G., Kress, J. M., and Jr, W. M.: Separation of Variables and Superintegrability The symmetry of solvable systems, IOP Publishing, https://doi.org/10.1088/978-0-7503-1314-8, 2018.

Kummer, E.: Über die hypergeometrische Reihe ... ., Journal für die reine und angewandte Mathematik, 15, 39–83, http://eudml.org/doc/146951, 1836.

Kurt M. Cuffey, W. S. B. P.: The Physics of Glaciers, Elsevier Science Techn., https://www.ebook.de/de/product/15174996/kurt_m_cuffey_w_s_b_paterson_the_physics_of_glaciers.html, 2010.

Lai, S.-H. and Jurinak, J.: Numerical approximation of cation exchange in miscible displacement through soil columns, Soil Science Society of America Journal, 35, 894–899, 1971.

Lie, S. and Scheffers, G.: Vorlesungen über continuierliche Gruppen mit geometrischen und anderen Anwendungen / Sophus Lie bearbeitet und herausgegeben von Georg Scheffers., B.G. Teubner,, https://doi.org/10.5962/bhl.title.18549, 1893.

Lliboutry, L.: Regime thennique et deformation de la base des calottes polaires, in: Annales de Geophysique, vol. 19, pp. 149–50, 1963.

MacAyeal, D. R.: Binge/purge oscillations of the Laurentide ice sheet as a cause of the North Atlantic's Heinrich events, Paleoceanography, 8, 775–784, 1993a.

MacAyeal, D. R.: A low-order model of the Heinrich event cycle, Paleoceanography, 8, 767–773, 1993b.

Marino, M. A.: Distribution of contaminants in porous media flow, Water Resources Research, 10, 1013–1018, https://doi.org/10.1029/wr010i005p01013, 1974.

Marshall, S. and Clarke, G.: A continuum mixture model of ice stream thermomechanics in the Laurentide Ice Sheet 2. Application to the Hudson Strait Ice Stream, Journal of Geophysical Research, 102, 20 615–20, 1997.

Marshall, T. J., Holmes, J. W., and Rose, C. W.: Soil Physics, Cambridge University Press, https://doi.org/10.1017/cbo9781139170673, 1996.

McLachlan, N.: Laplace Transforms and Their Applications to Differential Equations, Dover Books on Mathematics, Dover Publications, https://books.google.es/books?id=TDFeBAAAQBAJ, 2014.

Merks, R., Hoekstra, A., and Sloot, P.: The Moment Propagation Method for Advection–Diffusion in the Lattice Boltzmann Method: Validation and Péclet Number Limits, Journal of Computational Physics, 183, 563–576, https://doi.org/10.1006/jcph.2002.7209, 2002.

Meyer, C. and Minchew, B.: Temperate ice in the shear margins of the Antarctic Ice Sheet: Controlling processes and preliminary locations, Earth and Planetary Science Letters, 498, 17–26, https://doi.org/10.1016/j.epsl.2018.06.028, 2018.

Meyer, C. R., Robel, A. A., and Rempel, A. W.: Frozen fringe explains sediment freeze-on during Heinrich events, Earth and Planetary Science Letters, 524, 115 725, https://doi.org/10.1016/j.epsl.2019.115725, 2019.

Ogata, A.: Theory of dispersion in a granular medium, https://doi.org/10.3133/pp411i, 1970.

Ogata, A. and Banks, R. B.: A solution of the differential equation of longitudinal dispersion in porous media, 1961.

Perol, T. and Rice, J. R.: Control of the width of West Antarctic ice streams by internal melting in the ice sheet near the margins, in: AGU Fall Meeting Abstracts, vol. 2011, pp. C11B–0677, 2011.

Perol, T. and Rice, J. R.: Shear heating and weakening of the margins of West Antarctic ice streams, Geophysical Research Letters, 42, 3406–3413, https://doi.org/10.1002/2015gl063638, 2015.

Raymond, C. F.: Deformation in the Vicinity of Ice Divides, Journal of Glaciology, 29, 357–373, https://doi.org/10.3189/S0022143000030288, 1983.

Robel, A. A., DeGiuli, E., Schoof, C., and Tziperman, E.: Dynamics of ice stream temporal variability: Modes, scales, and hysteresis, Journal of Geophysical Research: Earth Surface, 118, 925–936, https://doi.org/10.1002/jgrf.20072, 2013.

Robin, G. d. Q.: Ice Movement and Temperature Distribution in Glaciers and Ice Sheets, Journal of Glaciology, 2, 523–532, https://doi.org/10.3189/002214355793702028, 1955.

Spikes, V. B., Hamilton, G. S., Arcone, S. A., Kaspari, S., and Mayewski, P. A.: Variability in accumulation rates from GPR profiling on the West Antarctic plateau, Annals of Glaciology, 39, 238–244, https://doi.org/10.3189/172756404781814393, 2004.

Stevens, C. M., Verjans, V., Lundin, J. M. D., Kahle, E. C., Horlings, A. N., Horlings, B. I., and Waddington, E. D.: The Community Firn Model (CFM) v1.0, Geoscientific Model Development, 13, 4355–4377, https://doi.org/10.5194/gmd-13-4355-2020, 2020.

Sturm, M., Holmgren, J., König, M., and Morris, K.: The thermal conductivity of seasonal snow, Journal of Glaciology, 43, 26–41, https://doi.org/10.3189/s0022143000002781, 1997.

Suckale, J., Platt, J. D., Perol, T., and Rice, J. R.: Deformation-induced melting in the margins of the West Antarctic ice streams, Journal of Geophysical Research: Earth Surface, 119, 1004–1025, https://doi.org/10.1002/2013jf003008, 2014.

Tulaczyk, S., Kamb, W. B., and Engelhardt, H. F.: Basal mechanics of Ice Stream B, west Antarctica: 2. Undrained plastic bed model, Journal of Geophysical Research: Solid Earth, 105, 483–494, https://doi.org/10.1029/1999jb900328, 2000b.

Zotikov, I. A.: The thermophysics of glaciers, https://www.osti.gov/biblio/5967995, 1986.